

TECHNICAL REPORT STANDARD TITLE PAGE

|   |  |  |  |
|---|--|--|--|
| 1. Report No.<br>FHWA/TX-87/77+401-6  | 2. Government Accession No.                          | 3. Recipient's Catalog No.   |  |
| 4. Title and Subtitle<br>FRICTION LOSSES IN UNBONDED<br>POST-TENSIONING TENDONS   |  | 5. Report Date<br>November 1986  | 6. Performing Organization Code                        |
| 7. Author(s)<br>Brian W. Dunn, Ned H. Burns,<br>and B. Frank McCullough   |  | 8. Performing Organization Report No.<br>Research Report 401-6   |  |
| 9. Performing Organization Name and Address<br>Center for Transportation Research<br>The University of Texas at Austin<br>Austin, Texas 78712-1075  |  | 10. Work Unit No.  | 11. Contract or Grant No.<br>Research Study 3-8-84-401 |
| 12. Sponsoring Agency Name and Address<br>Texas State Department of Highways and Public<br>Transportation; Transportation Planning Division<br>P. O. Box 5051<br>Austin, Texas 78763-5051   |  | 13. Type of Report and Period Covered<br>Interim   |  |
| 14. Sponsoring Agency Code  |  |  |  |
| 15. Supplementary Notes<br>Study conducted in cooperation with the U. S. Department of Transportation, Federal Highway Administration. Research Study Title: "Prestressed Concrete Pavement Design—Design and Construction of Overlay Applications"   |  |  |  |
| 16. Abstract<br><br>An important factor to be considered in the design of prestressed concrete pavements is the effective level of prestressing that the concrete feels. The effective prestress level must be high enough to prevent detrimental tensile stresses from developing in the concrete under service loads.<br>This study investigates the amount of the initial prestressing that is lost due to friction along the length of the post-tensioning tendons. Knowing the amount of friction losses that occur is essential in order to determine the effective prestress force at any point along the tendon.<br>Experimental tests were carried out on four test slabs with different configurations of unbonded post-tensioning tendons. The calculated losses were used to predict losses that would occur in an actual prestressed pavement. Friction losses measured during post-tensioning of the actual pavement were then compared to the calculated losses. |  |  |  |
| 17. Key Words<br>tendon, post-tensioning, unbonded, friction loss, prestress force, test slabs, prestressed concrete, design  |  | 18. Distribution Statement<br>No restrictions. This document is available to the public through the National Technical Information Service, Springfield, Virginia 22161. |  |
| 19. Security Classif. (of this report)<br>Unclassified  | 20. Security Classif. (of this page)<br>Unclassified | 21. No. of Pages<br>72   | 22. Price  |

**FRICTION LOSSES IN UNBONDED POST-TENSIONING TENDONS**

by

Brian W. Dunn  
Ned H. Burns  
B. Frank McCullough

Research Report 401-6

Prestressed Concrete Pavement Design - Design and Construction of Overlay Applications  
Research Project 3-8-84-401

conducted for

Texas State Department of Highways  
and Public Transportation

in cooperation with the  
U.S. Department of Transportation  
Federal Highway Administration

by the

Center for Transportation Research  
Bureau of Engineering Research  
The University of Texas at Austin

November 1986

The contents of this report reflect the views of the authors, who are responsible for the facts and the accuracy of the data presented herein. The contents do not necessarily reflect the official views or policies of the Federal Highway Administration. This report does not constitute a standard, specification, or regulation.

## PREFACE

This report is one of a series that describes work done under the project entitled "Prestressed Concrete Pavement Design - Design and Construction of Overlay Applications." The project is a joint effort by the Texas State Department of Highways and Public Transportation and the Center for Transportation Research at The University of Texas at Austin.

This report presents results from experimental tests carried out at Valley View, Texas, to determine friction losses in unbonded post-tensioning tendons. This study was carried out to determine the loss of prestress due to friction that could be expected in a demonstration of prestressed concrete overlay in McLennan County, Texas. Data collected during the construction of the overlay are also included in this report.

Special appreciation is extended to all project staff and to the rest of the Center for Transportation Research personnel for their assistance and invaluable contributions. Special thanks are extended to Alberto Mendoza, Neil Cable, Joe Maffei, and Scott O'Brien for their efforts in collecting the data. Dr. Muthu's guidance and advice during the project are also appreciated.

Blank Page

## LIST OF REPORTS

Report No. 401-1, "Very Early Post-tensioning of Prestressed Concrete Pavements," by J. Scott O'Brien, Ned H. Burns, and B. Frank McCullough, presents the results of tests performed to determine the very early post-tensioning capacity of prestressed concrete pavement slabs and gives recommendations for a post-tensioning schedule within the first 24 hours after casting.

Report No. 401-2, "New Concepts in Prestressed Concrete Pavement," by Neil D. Cable, Ned H. Burns, and B. Frank McCullough, presents the following: (a) a review of the available literature to ascertain the current state of the art of prestressed concrete pavement; (b) a critical evaluation of the design, construction, and performance of several FHWA sponsored prestressed concrete pavement projects which were constructed during the 1970s; and (c) several new prestressed concrete pavement concepts which were developed based on (a) and (b).

Report No. 401-3, "Behavior of Long Prestressed Pavement Slabs and Design Methodology," by Alberto Mendoza-Diaz, N. H. Burns, and B. Frank McCullough, presents the development of a model to predict the behavior of long prestressed concrete pavement (PCP) slabs and incorporate the predictions from the model into a design procedure.

Report No. 401-4, "Instrumentation and Behavior of Prestressed Concrete Pavements," by Joseph R. Maffei, Ned H. Burns, and B. Frank McCullough, describes the development and implementation of an instrumentation program used to monitor the behavior of a one-mile-long experimental prestressed concrete pavement and presents the results of measurements of ambient and concrete temperatures, horizontal slab movement, slab curling, concrete strain, very early concrete strength, concrete modulus of elasticity, and slab cracking.

Report No. 401-5, "Field Evaluation of Subbase Friction Characteristics," by Way Seng Chia, Ned H. Burns, and B. Frank McCullough, presents the results of push-off tests performed on four experimental test slabs at Valley View, Texas, to determine the maximum coefficient of friction of several friction reducing mediums for future implementation in the prestressed pavement projects in Cooke and McLennan counties.

Research Report No. 401-6, "Friction Losses in Unbonded Post-Tensioning Tendons," by Brian W. Dunn, Ned H. Burns, and B. Frank McCullough, presents results from experimental tests at Valley View, Texas, to determine friction losses in post-tensioning tendons to be used in the prestressed concrete pavement project in McLennan County, Texas. Collected data from the pavement project are also presented.

## ABSTRACT

An important factor to be considered in the design of prestressed concrete pavements is the effective level of prestressing that the concrete feels. The effective prestress level must be high enough to prevent detrimental tensile stresses from developing in the concrete under service loads.

This study investigates the amount of the initial prestressing that is lost due to friction along the length of the post-tensioning tendons. Knowing the amount of friction losses that occur is essential in order to determine the effective prestress force at any point along the tendon.

Experimental tests were carried out on four test slabs with different configurations of unbonded post-tensioning tendons. The calculated losses were used to predict losses that would occur in an actual prestressed pavement. Friction losses measured during post-tensioning of the actual pavement were then compared to the calculated losses.

Blank Page

## SUMMARY

Prior to construction of a prestressed concrete pavement overlay, experimental tests were performed to determine friction losses in post-tensioning tendons. The friction losses must be known to be able to determine the effective prestress level the concrete will feel. The tests were used to determine the friction coefficients for the tendons and the friction losses through the lock-coupler device.

During construction of the overlay, the tendon elongations and the jacking forces were measured for all of the tendons in the overlay. The data were used to calculate the actual amount of friction losses that occurred. Results of analysis on the data showed that greater friction losses occurred than were predicted from the results of the experimental tests.

Blank Page

## IMPLEMENTATION STATEMENT

This report presents recommendations that were made for determining friction losses in the unbonded post-tensioning tendons used in the demonstration prestressed concrete pavement overlay in McLennan County, Texas.

The recommended values for the wobble friction coefficient and the curvature friction coefficient were  $0.001 \text{ feet}^{-1}$  and  $0.07 \text{ radian}^{-1}$ , respectively. Data collected during construction of the McLennan County overlay indicate that these values should be  $0.001 \text{ feet}^{-1}$  and  $0.089 \text{ radian}^{-1}$ .

Blank Page

TABLE OF CONTENTS

PREFACE..... iii

LIST OF REPORTS..... v

ABSTRACT..... vii

SUMMARY..... ix

IMPLEMENTATION STATEMENT ..... xi

CHAPTER 1. INTRODUCTION

    OBJECTIVE OF THE REPORT ..... 1

    BACKGROUND ..... 1

CHAPTER 2. DESCRIPTION OF EXPERIMENTAL TESTS

    DESIGN OF TEST SLABS..... 7

    SITE PREPARATION..... 7

    CONSTRUCTION OF TEST SLABS ..... 13

    TESTING OF SLABS ..... 13

    POST-TENSIONING OF LOOPED TENDONS ..... 13

    CENTRAL STRESSING..... 18

CHAPTER 3. RESULTS OF EXPERIMENTAL TESTS

    TEST SLAB 1..... 21

    TEST SLAB 2..... 21

    TEST SLAB 3..... 21

    TEST SLAB 4..... 28

CHAPTER 4. ANALYSIS OF EXPERIMENTAL TEST SLAB RESULTS

    TENDON LAYOUTS..... 31

    FRICTION LOSSES..... 31

    TENDON STRESSING ..... 33

    LOCK-COUPLER..... 34

CHAPTER 5. TENDON LAYOUTS FOR THE McLENNAN COUNTY OVERLAY

    LONGITUDINAL TENDONS ..... 35

    TRANSVERSE TENDONS ..... 36

CHAPTER 6. DATA FROM McLENNAN COUNTY OVERLAY..... 39

CHAPTER 7. ANALYSIS AND DISCUSSION OF DATA

|                            |    |
|----------------------------|----|
| LONGITUDINAL TENDONS ..... | 43 |
| TRANSVERSE TENDONS .....   | 47 |
| DISCUSSION OF DATA .....   | 50 |

CHAPTER 8. CONCLUSIONS AND RECOMMENDATIONS

|                      |    |
|----------------------|----|
| CONCLUSIONS.....     | 53 |
| RECOMMENDATIONS..... | 54 |

|                  |    |
|------------------|----|
| REFERENCES ..... | 57 |
|------------------|----|

## CHAPTER 1. INTRODUCTION

### OBJECTIVE OF THE REPORT

Prior to construction of the prestressed concrete pavement overlay in McLennan County, Texas, experimental tests were performed to evaluate the performance of materials to be used in the overlay. This report in part is intended to present the results of these tests. Also presented in this report are observed data recorded during the actual construction of the one mile of overlay in McLennan County. Analysis of these data will show how the materials performed in the pavement construction compared to the behavior observed in the smaller scale experimental tests (Ref 1).

### BACKGROUND

The experimental tests were performed to provide information on the amount of friction loss that occurs in different types of unbonded post-tensioning tendons. Two types of plastic coated tendons were tested in several tendon configurations. Looped configurations involving different angle changes were examined as well as straight tendons.

Analysis of looped tendons was necessary since some of the alternatives proposed for providing transverse post-tensioning on the McLennan County overlay require the looping of the tendons. Figure 1.1 shows one alternative with the advantage that four transverse tendons can be stressed through an internal stressing pocket in one post-tensioning operation. Stressing pockets are described later in this chapter.

The frictional losses in all post-tensioning tendons can be divided into two parts: the length effect and the intended curvature effect. The length effect is the amount of friction that would be encountered if the tendon were intended to be straight (any curvature is created during construction and is unintended). This frictional loss is dependent on the length and stress of the tendon, the method used in aligning it prior to the casting of the concrete, and the coefficient of friction between the contact materials. The length effect can be substantially reduced by using tendons which are lubricated and encased in flexible thin wall plastic coating. The loss of prestress due to intended curvature is also dependent on the coefficient of friction between the contact materials as well as the pressure exerted by the tendon on the concrete as

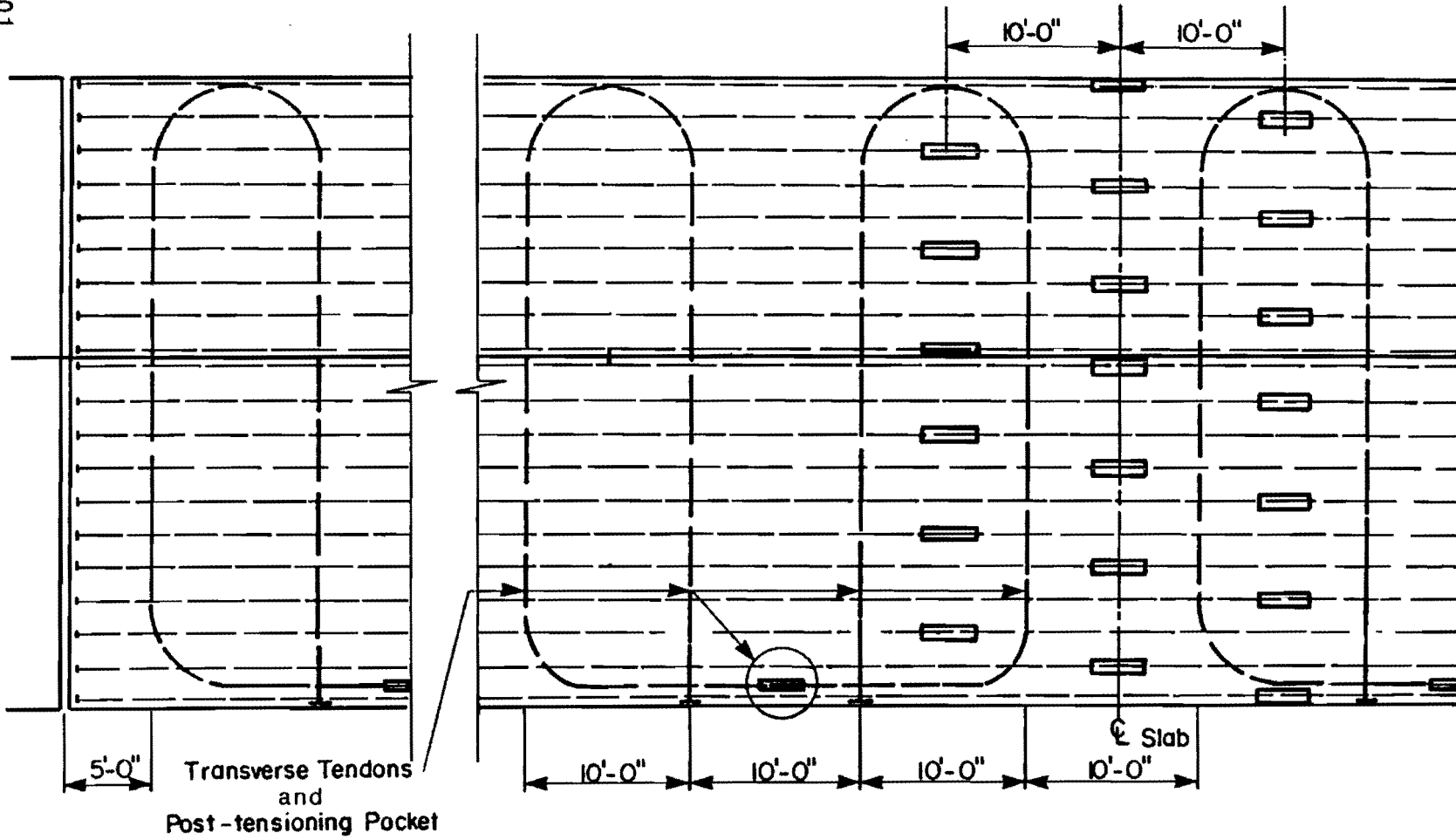


Fig 1.1. Alternative for providing transverse post-tensioning.

a result of the total angle change. The formula proposed by the 1983 ACI Building Code Requirements for Reinforced Concrete (Ref 2) to compute the friction losses due to the length and curvature effects is

$$P_s = P_x e^{(kl_x + \mu\alpha)} \quad (1.1)$$

where

- $P_s$  = prestressing tendon force at jacking end, in kips,
- $P_x$  = prestressing tendon force at any point X, in kips,
- $K$  = wobble friction coefficient per foot of prestressing tendon,
- $l_x$  = length of prestressing tendon from jacking end to any point X, in feet,
- $\mu$  = curvature friction coefficient, and
- $\alpha$  = total angular change of prestressing tendon from jacking end to any point X, in radians.

In the experimental tests, the losses produced in loops of 180, 270, and 720° were analyzed for two different types of plastic coated tendons. These tendon types are identified as I and II throughout this report. Both tendon types were provided with plastic coating; however the 36-mil coating on the Type I tendons was in much better condition than the coating on the Type II tendons. The coating on the Type II tendons was damaged during transportation and handling, and its thickness was less than that for Type I tendons.

One important aspect of the experimental tests was the investigation of methods of post-tensioning the tendons. One method consists of stressing the tendons at internal blockouts or stressing pockets which are then filled with concrete after the post-tensioning force has been applied. In this method of post-tensioning, the stressing pocket is located at an interior point within the slab, with the two segments of the tendon extending from the pocket to anchors set in each end of the slab. The two segments of the tendon overlap in the stressing pockets and are inserted through a steel sleeve, known as a lock-coupler, as shown in Fig 1.2. Anchorages are installed on the protruding tendon ends and the stressing ram is then attached to end A of segment 1 of the tendon. Both segments are simultaneously stressed as the prestress force is applied by the hydraulic jacking device.

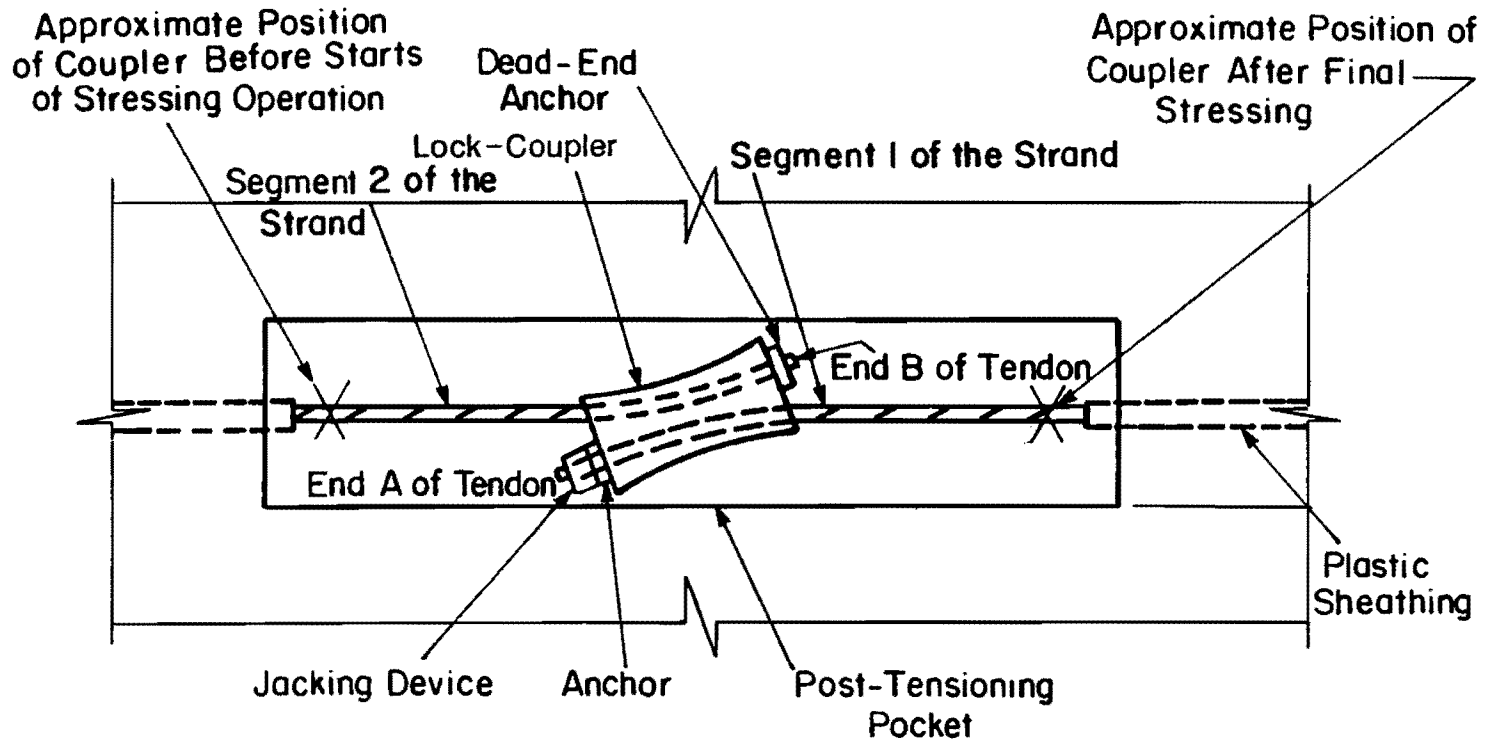


Fig 1.2. Post-tensioning pocket detail.

The tests, in part, were conducted so as to quantify the amount of friction loss generated through the lock-coupler device during stressing. This information, combined with the information on friction losses due to the length and curvature effects, will enable the total losses due to friction to be quantified.

The experimental tests were also conducted to investigate the following additional items:

- (1) the effectiveness of several different materials in relieving the frictional forces that develop at the interface of the prestressed slab and its underlying support, and
- (2) alternate techniques of post-tensioning the longitudinal tendons through internally located stressing pockets.

Tests concerning these two items were conducted at the same time the tests for frictional losses were performed. Item 2 is briefly discussed later in this report. Analysis and discussion of Item 1 is the topic of another report, "Field Evaluation of Subbase Friction Characteristics" (Ref 3).

In addition to conducting the experimental tests, the actual performance of the post-tensioned tendons used in the one mile long overlay constructed in McLennan County were recorded. During the post-tensioning operation, the tendon elongation and the jacking force was measured and recorded. Knowing the size, length, and layout of the tendons as well as the elongations and jacking force enables the wobble coefficient,  $k$ , and the curvature coefficient,  $m$ , to be back calculated. A comparison between the coefficients predicted by the experimental tests and the back calculated coefficients is useful in developing a reliable method for predicting frictional losses for prestressed pavements.

This page replaces an intentionally blank page in the original.

-- CTR Library Digitization Team

## CHAPTER 2. DESCRIPTION OF EXPERIMENTAL TESTS

### DESIGN OF TEST SLABS

The testing of four experimental slabs served as the basis for the study of prestress losses due to friction. Figures 2.1, 2.2, 2.3, and 2.4 show the test slabs as they were originally designed.

The four 6-inch-thick test slabs were designed specifically for analyzing the following:

Test Slab 1: (1) The friction losses produced in the Type I tendons (plastic coating in good condition) when stressed through a loop of 180° and (2) the friction losses generated through the lock-coupler during application of the post-tensioning force.

Test Slab 2: The friction losses produced in Type II tendons (plastic coating in poor condition) when stressed through a loop of 180°.

Test Slab 3: The friction losses generated in Type II tendons when stressed through a loop of 270°.

Test Slab 4: The friction losses generated in Type I tendons when stressed through a loop of 720°.

### SITE PREPARATION

The test slabs were constructed on May 15-16, 1984. The test site was located approximately 1-1/2 miles south of Valley View, Texas. Prior to the construction of the slabs, the site was prepared to provide a smooth and uniform asphalt surface. Figure 2.5 shows a sand mix asphalt pad laid for this purpose on top of the subgrade. Then, the locations of the slabs along the asphalt pad were marked with spray paint. Preparations were then made for aspects of the tests involving frictional forces at the interface of the slab and the supporting pad.

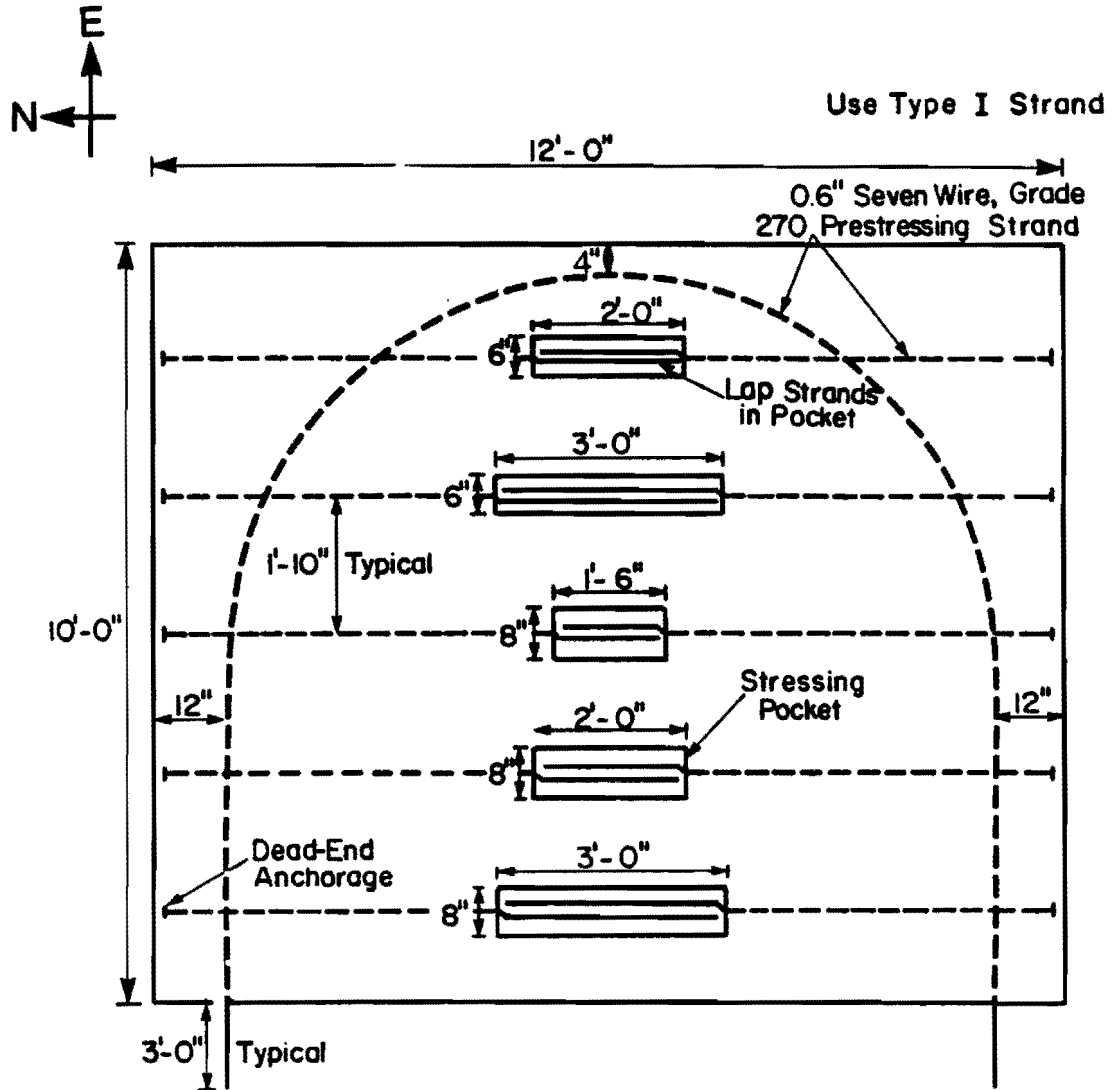


Fig 2.1. Test Slab No. 1.



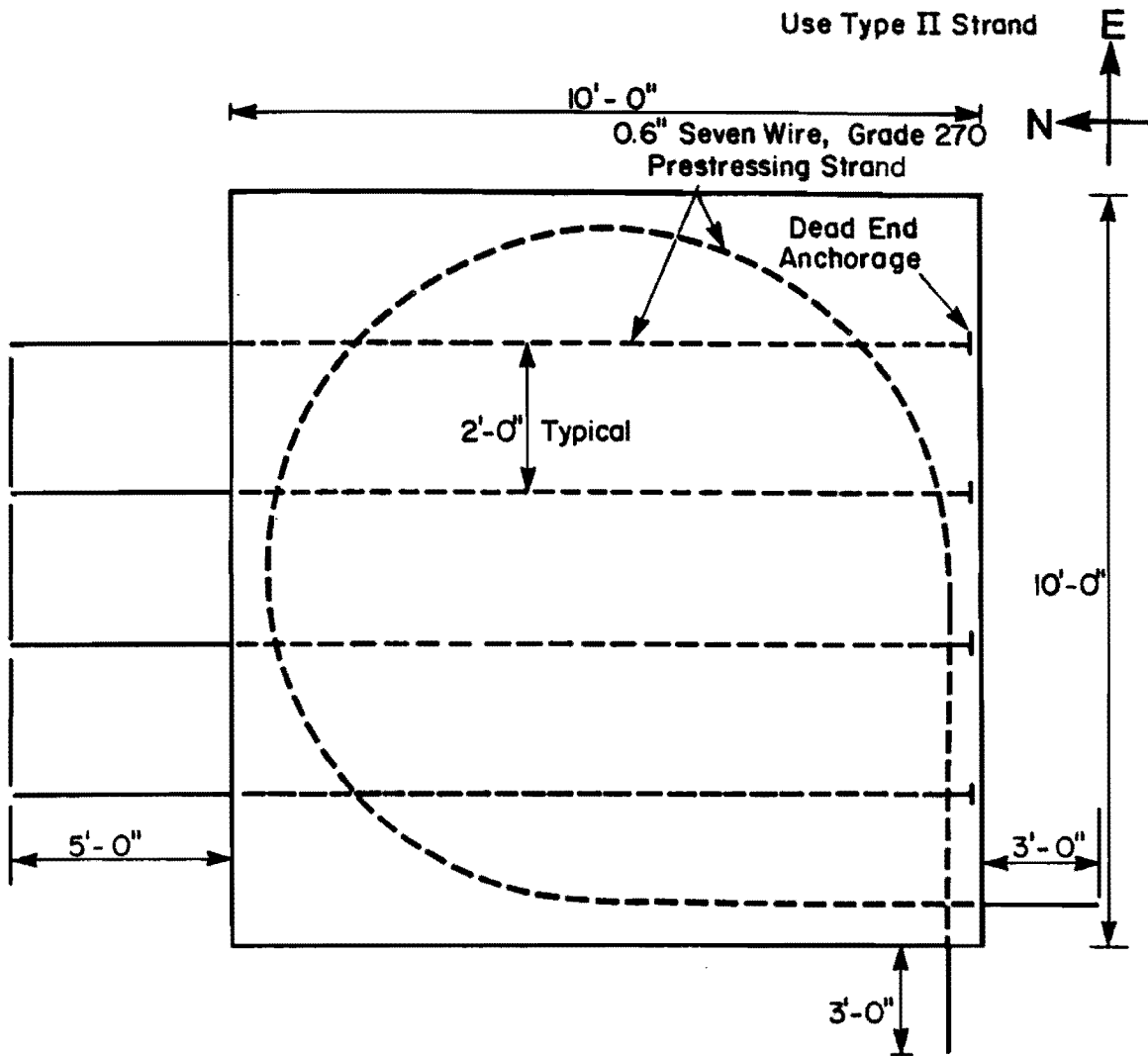


Fig 2.3. Test Slab No. 3.

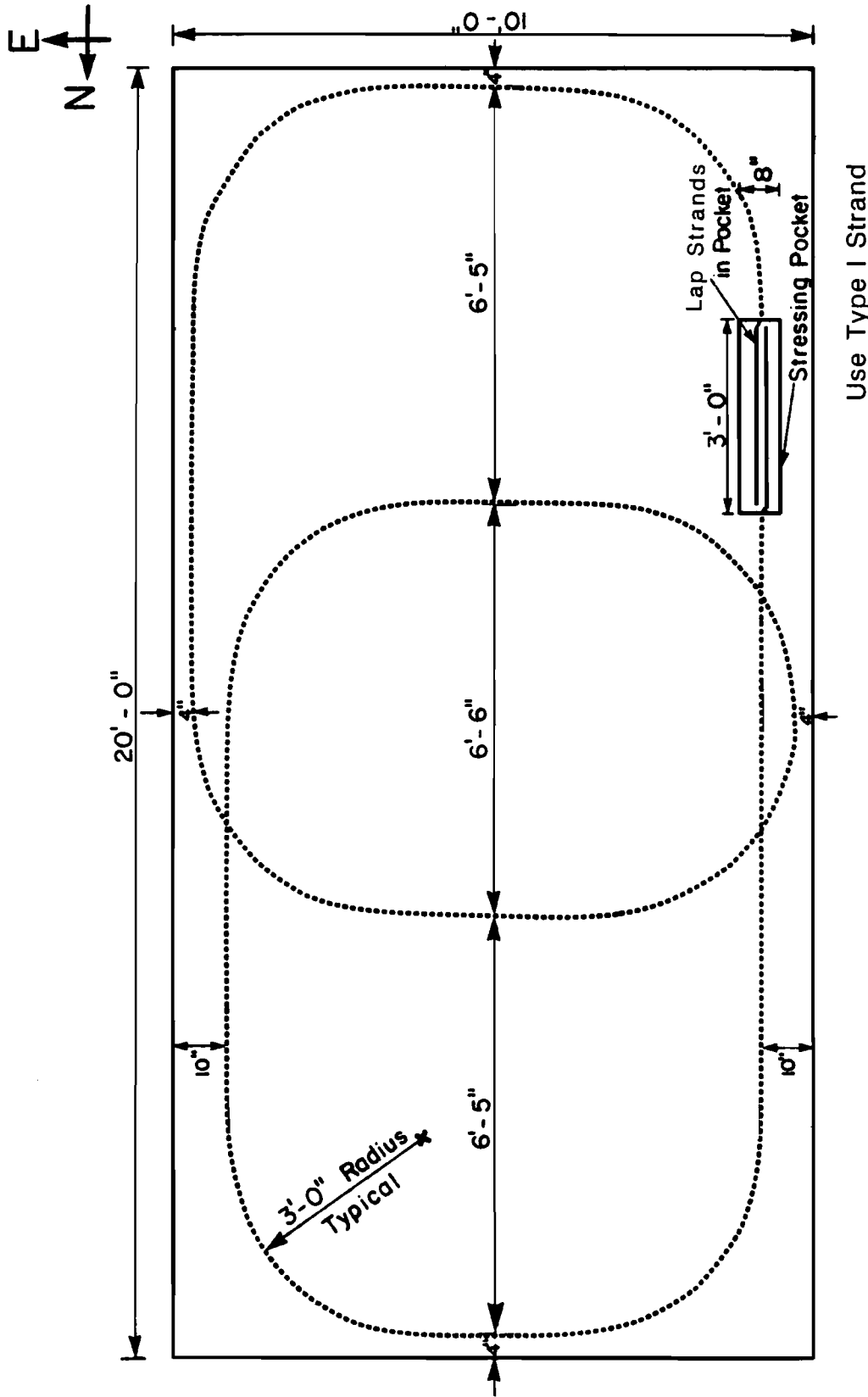


Fig 2.4. Test Slab No. 4.



Fig 2.5. Sand mix asphalt pad prepared to provide a smooth surface for the test slabs.

## CONSTRUCTION OF TEST SLABS

First, the formwork for each slab was prepared as shown in Fig 2.6. The tendons were then put in place inside the formwork and secured with tie wires at points of intersection of crossing strands. The wood boxes for the blockouts were placed at the required locations and secured in place by boards nailed to the top of the slab formwork and the top of the boxes. The final arrangements of Test Slabs 1, 2, 3, and 4 before casting of the concrete are presented in Figs 2.7, 2.8, 2.9, and 2.10, respectively.

Casting of the concrete was done on May 16, 1984. The four test slabs were cast, vibrated, screeded, and trowel finished. Three different concrete deliveries were used for casting the slabs. After trowel finishing all slabs, the exposed slab surfaces were sprayed with a curing compound. Figure 2.11 shows a general view of the test site after casting of the slabs.

## TESTING OF SLABS

All tests on the slabs were conducted on May 31 and June 1, 1984. Subbase friction results are described in Ref 3 and are included here. By the date of testing, the concrete strength was approximately  $f'_c \cong 5000$  psi and this was not a factor in the analysis of either base friction or tendon friction coefficients.

## POST-TENSIONING OF LOOPED TENDONS

The looped tendons in the test slabs were post-tensioned using a VSL stressing ram. The tendon was anchored at one end while being jacked from the other. Load cells were placed on both ends of the looped tendon to determine the forces transmitted to the concrete at the tendon ends and to quantify the amount of friction losses through the curved portion of the tendon path. The tendon was post-tensioned at the initial stressing end to 80 percent of its ultimate strength. The elongation of the tendons and the readings on the load cells were taken during application of the post-tensioning force. For the looped tendon in Test Slab 4, the



Fig 2.6. Preparation of formwork for slabs.



Fig 2.7. Layout of Test Slab No. 1 before the concrete was cast.

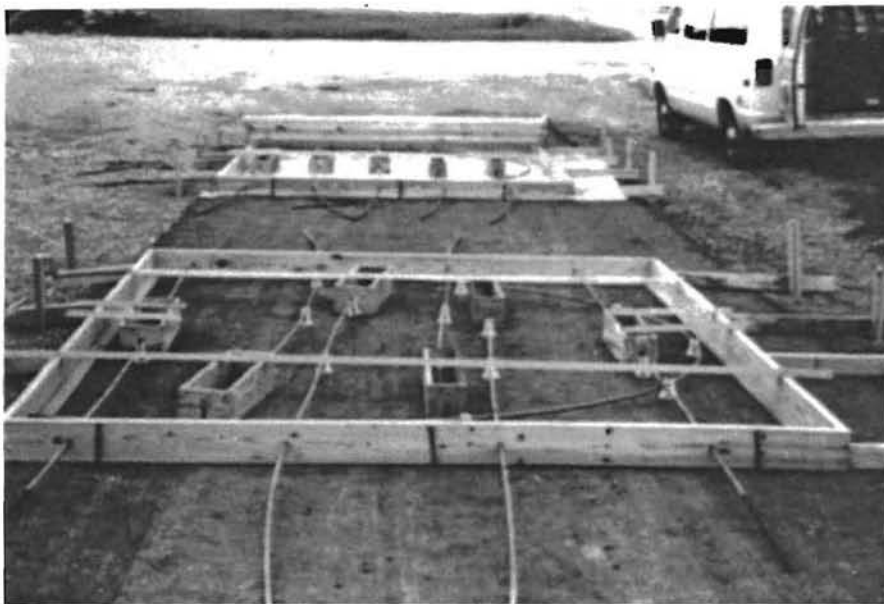


Fig 2.8. Layout of Test Slab No. 2 before the concrete was cast.

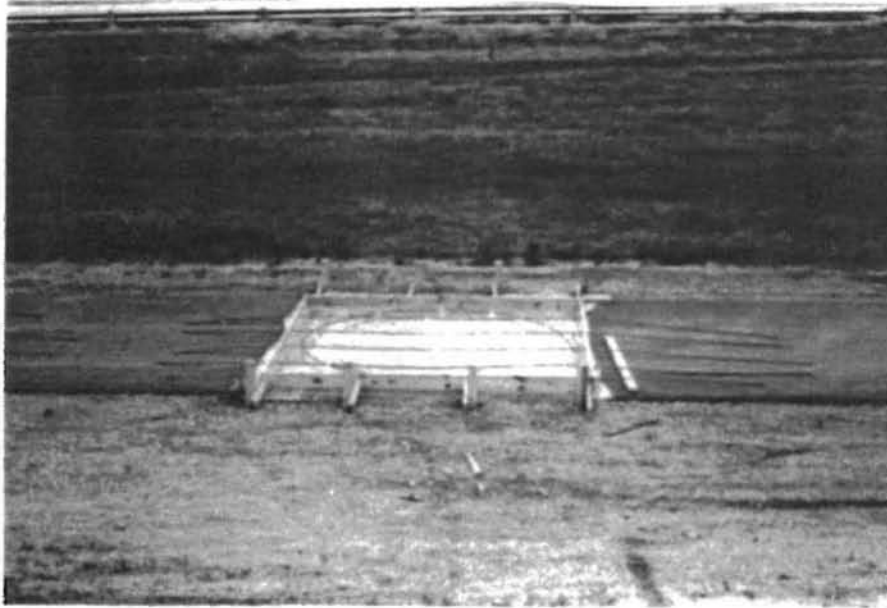


Fig 2.9. Layout of Test Slab No. 3 before the concrete was cast.

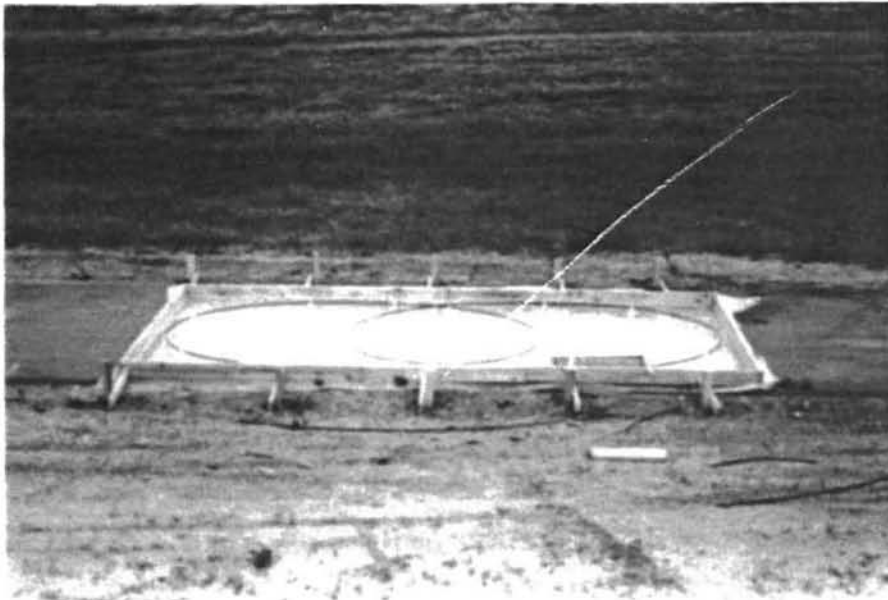


Fig 2.10. Layout of Test Slab No. 4 before the concrete was cast.



Fig 2.11. General view of the test site after the slabs were cast.

post-tensioning force was applied through an internal stressing pocket of 8 x 36 inches. The stressing operation is described in more detail in a later section of this report. A general view of the post-tensioning operation of the looped tendon of Test Slab 1 is shown in Fig 2.12.

#### CENTRAL STRESSING

The dimensions of the central stressing pockets shown in Figs 2.1, 2.2, 2.3, and 2.4 were defined based on the dimensions of a typical VSL stressing ram as presented in the Post Tensioning Institute's Post-tensioning Manual (Ref 4). However, the dimensions of the actual stressing ram obtained from VSL were considerably larger than those shown in the manual and it would have been extremely difficult to post-tension in pockets smaller than 6 x 36 inches. Therefore, the central stressing was performed only on the 6 x 36 inch and the 8 x 36 inch pockets of Test Slab 1 and on the 8 x 36 inch pocket of Test Slab 4.

The tendons in Test Slab 1 were stressed by jacking both segments of the tendon using a lock-coupler device (Fig 1.2) within the stressing pocket. Load cells were installed at each of the other ends of the tendon segments in order to determine the friction losses generated through the lock-coupler device. Figure 2.13 shows the extended ram stressing the tendon in one of the pockets of Test Slab 1.

The tendon in Test Slab 4 was stressed by anchoring one end while jacking the tendon from the other end. A load cell was placed on the anchored end in order to determine the friction losses generated through the 720° loop. Figure 2.14 illustrates the orientation of the ram which was necessary in order to stress the looped tendon in Test Slab 4.

All tendons were post-tensioned at the stressing end to 80 percent of their ultimate strength.



Fig 2.12. Post-tensioning operation of looped strand of Test Slab No. 1.

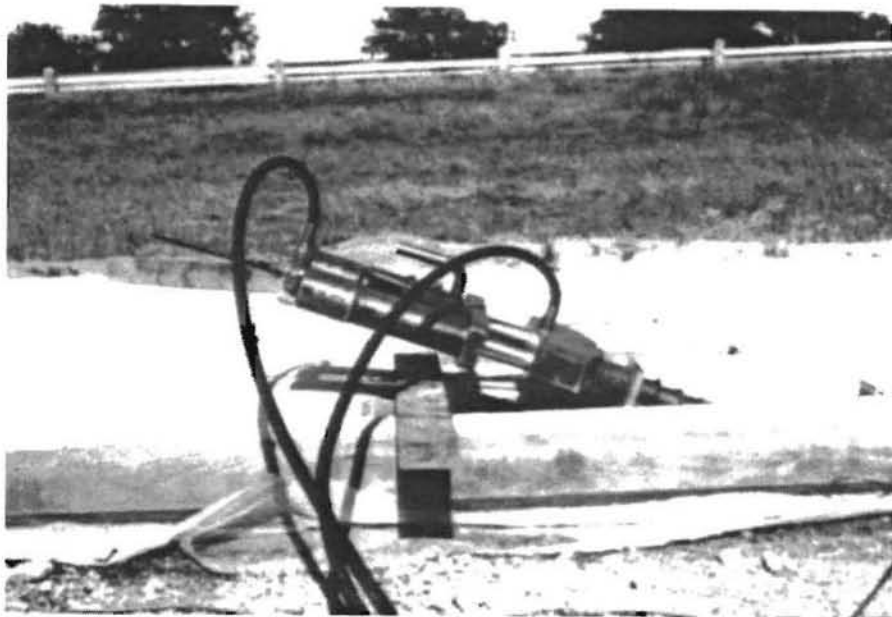


Fig 2.13. Stressing of the tendon in the 8 x 36-inch pocket of Test Slab No. 1.

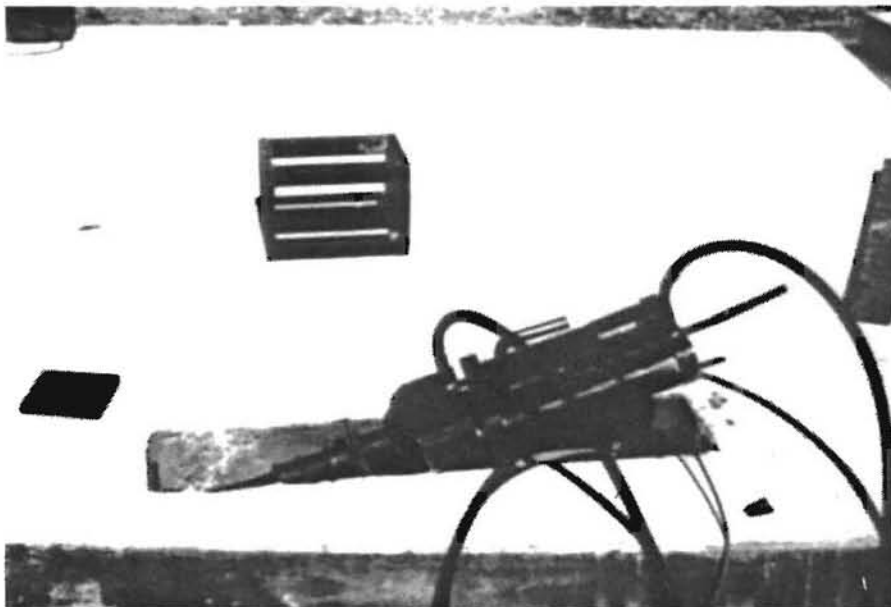


Fig 2.14. Orientation of stressing ram required to post-tension the looped strand of Test Slab No. 4 in the 8 x 36-inch pocket.

## CHAPTER 3. RESULTS OF EXPERIMENTAL TESTS

### TEST SLAB 1

Figure 3.1 shows the tendon layout that could be obtained in the field that was closest to the one originally proposed in Fig 2.1. The actual layout is very close to the proposed one.

The looped tendon post-tensioning test was performed twice. The forces on the jacked end of the tendon (initial end) and on the anchored end (final end) are reported in Table 3.1, along with the frictional losses  $DP$  and the calculated average from the two runs. Table 3.1 shows the corresponding elongations, measured at the initial end of the tendon, and the theoretical values determined from linear elasticity. The average elongations, measured and computed, are also shown.

The central stressing test was run twice for the tendons marked (a) and (b) in Fig 3.1. Table 3.2 presents the values of the force  $P_{initial}$  applied on the jacked segment of the tendon at the lock-coupler and the forces  $P_{final}$  read at the other ends of the two segments. It should be kept in mind that, in the lock-coupler system of central post-tensioning, one of the segments of the tendon is jacked directly whereas the other segment is stressed indirectly at the same time.

### TEST SLAB 2

Figure 3.2 shows the tendon layout that could be obtained in the field that was closest to the one originally proposed in Fig 2.2. The actual layout is very close to the proposed one. Table 3.3 shows the friction losses and elongations obtained from post-tensioning the 180° looped tendon.

### TEST SLAB 3

Figure 3.3 shows the tendon layout that could be obtained for the 270° looped tendon that was closest to the one originally proposed in Fig 2.3. The actual layout is very close to the proposed one. Table 3.4 shows the friction losses and elongations obtained from the post-tensioning of the 270° looped tendon.

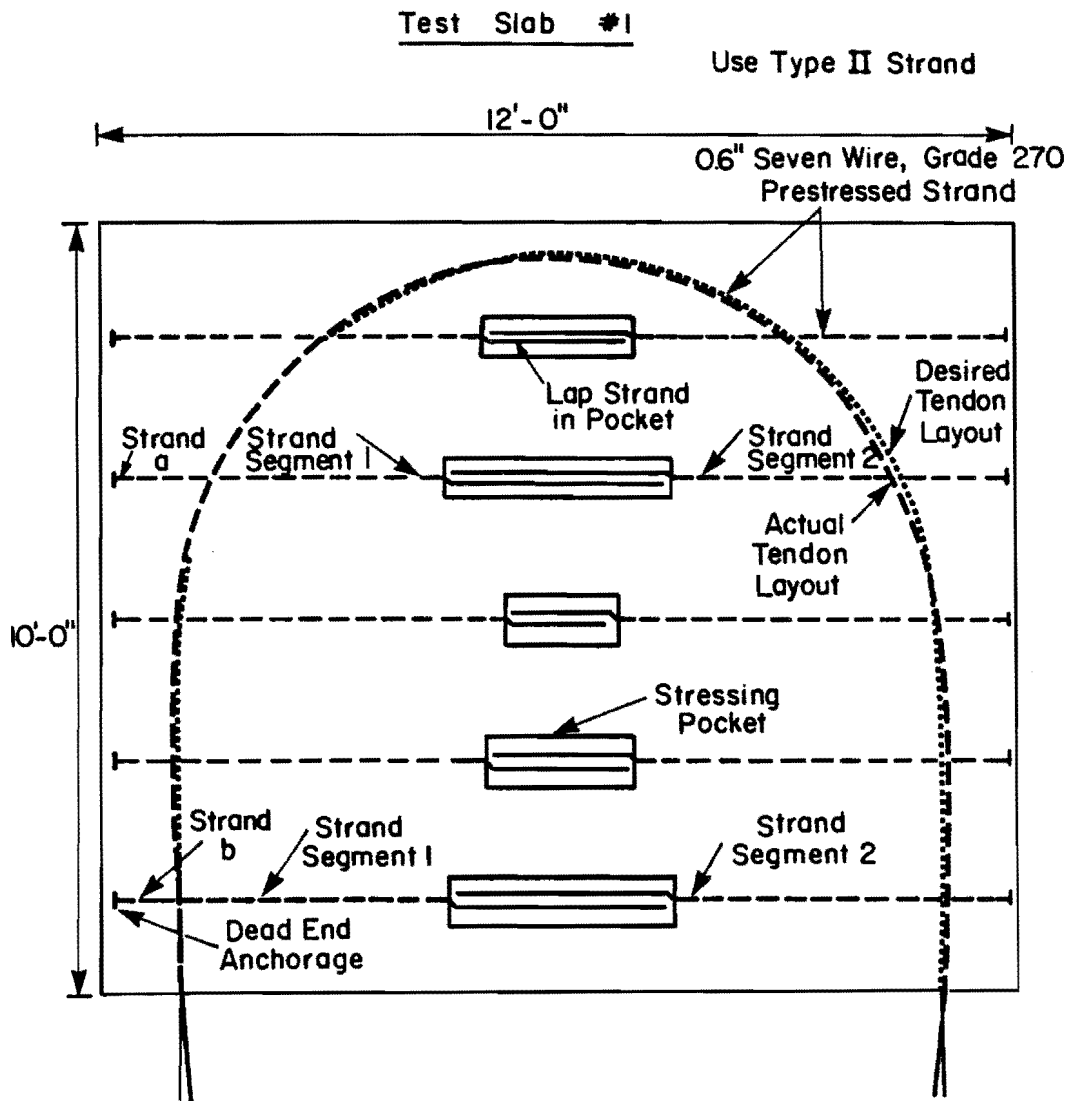


Fig 3.1. Actual layout obtained in the field for Test Slab 1.

TABLE 3.1. FRICTIONAL LOSSES AND ELONGATIONS OF LOOPED STRAND (TEST SLAB 1)

| Run     | Force on<br>Initial End | Force on<br>Final End | Loss $\Delta P$ | Measured<br>Elongation<br>(in.) | Theoretical<br>Elongation<br>(in.) |
|---------|-------------------------|-----------------------|-----------------|---------------------------------|------------------------------------|
| 1       | 46.8 k                  | 42.3 k                | 4.5 k           | 2.40                            | 2.34                               |
| 2       | 46.8 k                  | 42.8 k                | 4.0 k           | 2.50                            | 2.35                               |
| Average | 46.8                    | 42.55                 | 4.25            | 2.45                            | 2.345                              |

Note: Post-tensioning of Looped Strand Results  
(180° Loop - Type I Tendon)

TABLE 3.2. FRICTIONAL LOSSES THROUGH THE LOCK-COUPLER

| Strand | Run     | Lock-Coupler | At the Other End of<br>Segment of Strand Being Pulled |            | At the End of the<br>Other Segment of Strand |            |
|--------|---------|--------------|---|------------|--|------------|
|        |         |              | $P_{\text{final}}$                                    | $\Delta P$ | $P_{\text{final}}$                           | $\Delta P$ |
| A      | 1       | k<br>46.8    | k<br>43.99  | k<br>2.81  | k<br>42.47                                   | 4.33       |
|        | 2       | k<br>46.8    | k<br>44.12  | k<br>2.68  | k<br>42.52                                   | 4.28       |
| B      | 1       | k<br>46.8    | k<br>44.86  | k<br>1.94  | k<br>42.75                                   | 4.05       |
|        | 2       | k<br>46.8    | k<br>44.25  | k<br>2.55  | k<br>42.66                                   | 4.14       |
|        | Average | k<br>46.8    | k<br>44.31  | k<br>2.50  | k<br>42.60                                   | 4.20       |

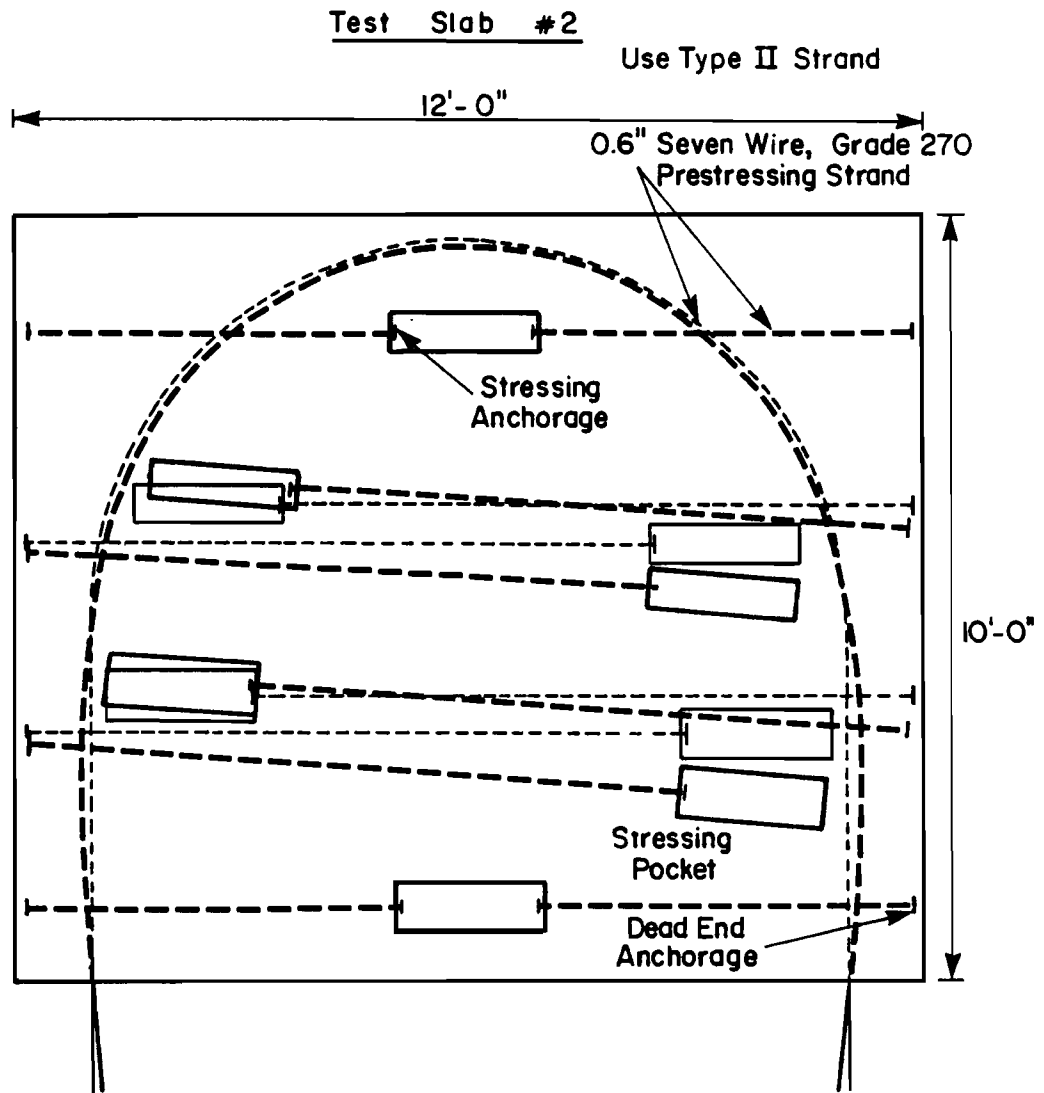


Fig 3.2. Actual layout obtained in the field for Test Slab 2.

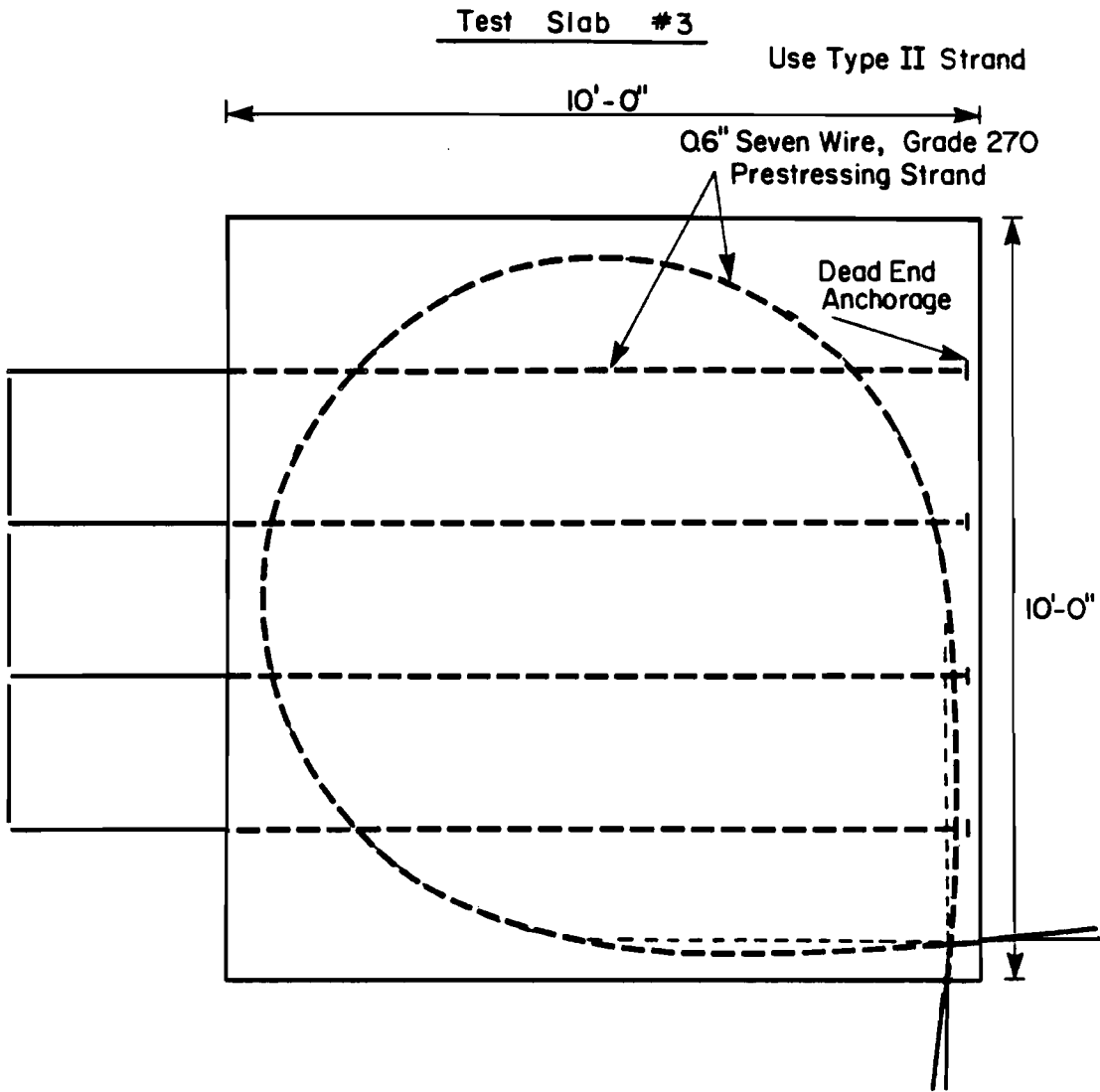


Fig 3.3. Actual layout obtained in the field Test Slab 3.

TABLE 3.3. FRICTIONAL LOSSES AND ELONGATIONS OF LOOPED STRAND (TEST SLAB 2)

| Run     | Force on<br>Initial End | Force on<br>Final End | Loss $\Delta P$ | Measured<br>Elongation<br>(in.) | Theoretical<br>Elongation<br>(in.) |
|---------|-------------------------|-----------------------|-----------------|---------------------------------|------------------------------------|
| 1       | 46.8 k                  | 37.9 k                | 8.9 k           | 2.84                            | 2.22                               |
| 2       | 46.1 k                  | 37.9 k                | 8.2 k           | 2.44                            | 2.20                               |
| Average | 46.45 k                 | 37.9 k                | 8.55 k          | 2.64                            | 2.21                               |

Note: Post-tensioning of Looped Strand Results  
(180° Loop - Type II Tendon)

## TEST SLAB 4

Figure 3.4 shows the tendon layout that could be obtained in the field that was closest to the one originally proposed in Fig 2.4. The actual layout is significantly different from the proposed one due to the stiffness of the 0.6-inch-diameter tendon. A 0.5-inch-diameter tendon would not be as stiff and could be laid out closer to the proposed layout. Table 3.5 shows the friction losses and elongations obtained from the post-tensioning of the 720° looped tendon.

TABLE 3.4. FRICTIONAL LOSSES AND ELONGATIONS OF LOOPED STRAND (TEST SLAB 3)

| Run     | Force on Initial End | Force on Final End | Loss $\Delta P$ | Measured Elongation (in.) | Theoretical Elongation (in.) |
|---------|----------------------|--------------------|-----------------|---------------------------|------------------------------|
| 1       | k<br>45.97           | k<br>34.56         | k<br>11.41      | 3.50                      | 2.38                         |
| 2       | k<br>45.6            | k<br>35.26         | k<br>10.34      | 2.91                      | 2.39                         |
| Average | k<br>45.78           | k<br>34.91         | k<br>10.88      | 3.20                      | 2.39                         |

Note: Post-tensioning of Looped Strand Results  
(270° Loop - Type II Tendon)

TABLE 3.5. FRICTIONAL LOSSES AND ELONGATIONS OF LOOPED STRAND (TEST SLAB 4)

| Run     | Force on Initial End | Force on Final End | Loss $\Delta P$ | Measured Elongation (in.) | Theoretical Elongation (in.) |
|---------|----------------------|--------------------|-----------------|---------------------------|------------------------------|
| 1       | k<br>46.0            | k<br>32.87         | k<br>13.13      | 6.38                      | 5.28                         |
| 2       | k<br>46.0            | k<br>33.65         | k<br>12.35      | 5.38                      | 5.33                         |
| Average | k<br>46.0            | k<br>33.26         | k<br>12.74      | 5.88                      | 5.31                         |

Note: Post-tensioning of Looped Strand Results  
(720° Loop - Type I Tendon)

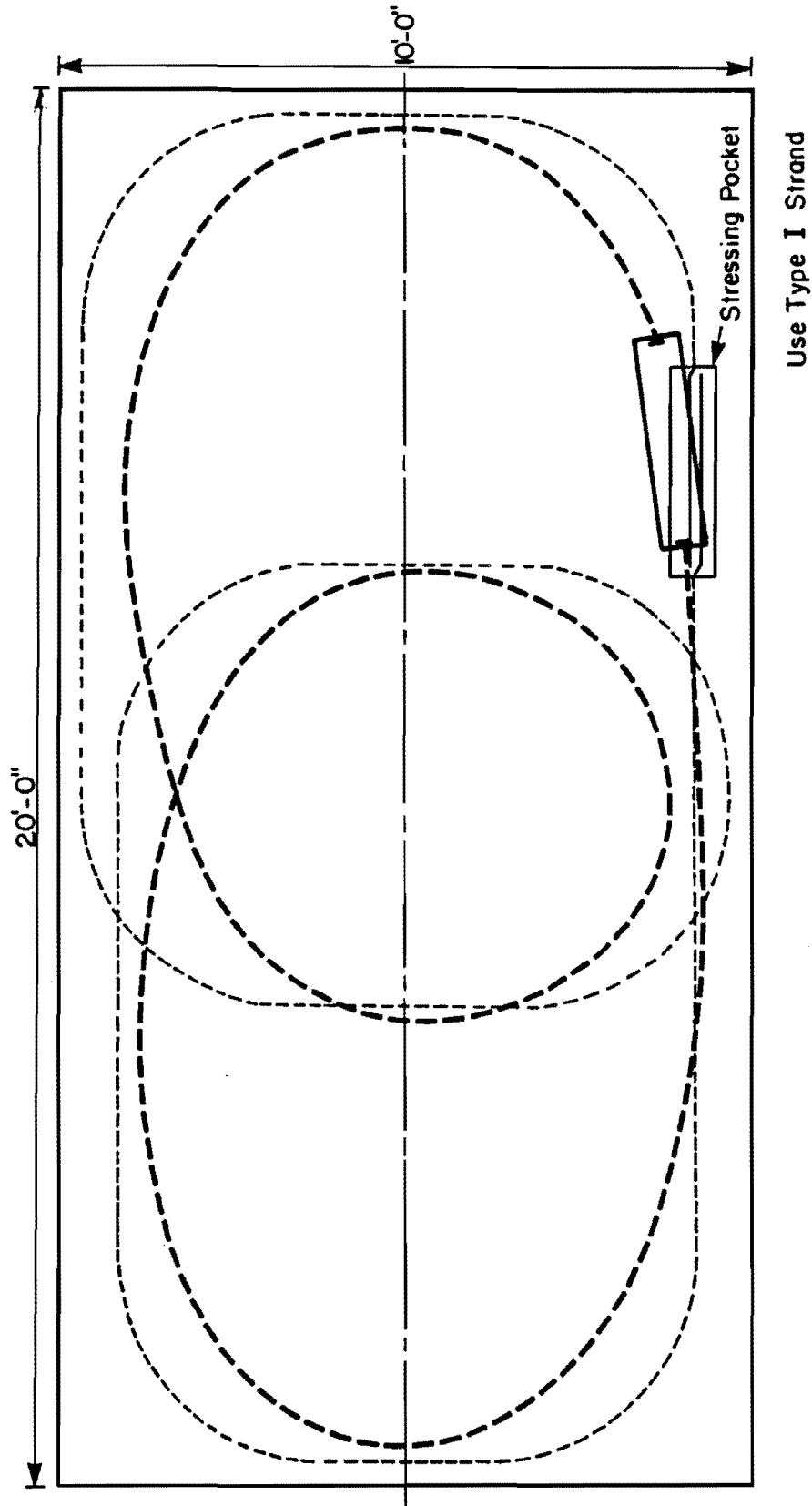


Fig 3.4. Actual layout obtained in the field for Test Slab 4.

## CHAPTER 4. ANALYSIS OF EXPERIMENTAL TEST SLAB RESULTS

The following points can be made based on the results of the experimental tests of the four slabs described in the previous chapters. The values presented for the friction coefficients are those given in Ref 1.

### TENDON LAYOUTS

The tendon layouts proposed for the looped tendons as presented in Figs 2.1, 2.2, 2.3, and 2.4, could not be obtained as originally designed. The closest tendon layouts that could be obtained in the field are shown in Figs 3.1, 3.2, 3.3, and 3.4. The 0.6-inch diameter tendons were not flexible enough to allow sharp radius loops and they had to be tied in place in all the cases to maintain the required shape. Some difficulties might occur during placement of long segments of tendon that are in looped configurations similar to the one shown in Fig 1.1. In these cases it is recommended that the required shape be given to the tendons by using ties to form the loops prior to placing them inside the formwork.

### FRICITION LOSSES

Table 4.1 is a summary of the frictional losses generated in the looped tendons during application of the post-tensioning force. The lengths of the tendons and the angle changes involved are also shown in Table 4.1. Table 4.2 presents the wobble friction coefficient and the curvature friction coefficient derived by applying Eq 1.1 to the results shown in Table 4.1. It can be seen that the friction coefficients for Type II tendons are almost twice as much as the friction coefficients for Type I tendons.

The theoretical tendon elongations for the McLennan County overlay were calculated using a wobble coefficient of  $0.001 \text{ foot}^{-1}$  and a curvature coefficient of  $0.07 \text{ radian}^{-1}$ . These values are within the recommended ranges of values given in Ref 5 and were used only to estimate the elongations.

TABLE 4.1. SUMMARY OF FRICTION LOSSES THROUGH THE LOOPED STRANDS

| Test Slab Number | Tendon Type | Strand Length (feet) | Angle Change (°) | Frictional Loss $\Delta P(K)$ |
|------------------|-------------|----------------------|------------------|-------------------------------|
| 1                | I           | 25.83                | 180              | 4.25                          |
| 2                | II          | 25.83                | 180              | 8.55                          |
| 3                | II          | 29.17                | 270              | 10.88                         |
| 4                | I           | 64.33                | 720              | 12.74                         |

TABLE 4.2. LENGTH AND CURVATURE COEFFICIENTS  $\mu$  AND  $K$  FOR TENDON TYPES I AND II TESTED IN EXPERIMENT

| Tendon Type | Length Coefficient, $K$ (per foot) | Curvature Coefficient, $\mu$ (per radian) |
|-------------|------------------------------------|---|
| I           | 0.00145                            | 0.0184                                    |
| II          | 0.00356                            | 0.0355                                    |

It is recommended that good condition of the plastic coating be insured, especially if the tendons will be placed in looped configurations. Also, good quality plastic material is required for the coating in order to minimize the damage to it during transportation and handling. A minimum plastic coating thickness of 36 mils should be specified for looped tendons. In straight tendons, thinner plastic coatings might be used, but thicknesses thinner than 30 mils should not be allowed.

Finally, a check of the elongation of the looped tendons during application of the post-tensioning force against the computed theoretical elongations indicates that the tendons were uniformly stressed along the entire tendon length. It is recommended that this kind of a check be used during post-tensioning operations to ensure that the tendon is stressed to the required level.

#### TENDON STRESSING

In the central stressing schemes, the pocket width must be large enough to provide at least 1/4 inch of clearance on both sides of the stressing ram. For the central stressing scheme that does not use the lock-coupler device, the pocket length need only be long enough to accommodate the tendon anchors and the fully extended ram. Therefore, the required pocket size is dependent on the size of the stressing ram to be used. For the scheme where the lock-coupler device is used, the position of the lock-coupler changes in response to the application of the prestress force and the tendon elongation. Therefore, the pocket length must accommodate not only the fully extended ram but also the lock-coupler movement. In this case, the required stressing pocket size is dependent on the size of the stressing ram and the anticipated tendon elongation. The anticipated tendon elongation depends on the length of the tendon and the force applied.

Stressing in properly sized pockets would be only slightly more difficult than stressing the tendons at the edge of the slab. This increase in difficulty is attributable to a more confined working space. It is important to know the dimensions of the stressing rams that will actually be used during construction to permit the proper sizing of the stressing pockets. Any discrepancies could result in extra work being required to enlarge stressing pockets that are too small. Since equipment dimensions vary, it is impossible to set absolute dimensions for the stressing pockets.

## LOCK-COUPLER

Data concerning the friction losses generated through the lock-coupler device proved to be inconclusive. The data shown in Table 3.2 indicate that the force in one segment of the tendon is greater than the force in the other segment. In a free-body analysis of the lock-coupler device, the forces in the two segments of the tendon are required to be equal if static equilibrium is to be satisfied. In determining the jacking force required to provide the minimum effective prestress level in the concrete, the friction losses need to be estimated. The theoretical tendon elongations for the McLennan County overlay were calculated assuming that the wobble and curvature coefficients took into account the friction losses through the lock-coupler.

## CHAPTER 5. TENDON LAYOUTS FOR THE McLENNAN COUNTY OVERLAY

The layout of the tendons for the McLennan County overlay includes straight tendons for prestressing the concrete in the longitudinal direction and looped tendons for prestressing in the transverse direction (see Fig 1.1). All the tendons were post-tensioned from internally located stressing pockets with the use of lock-coupler devices.

### LONGITUDINAL TENDONS

The overlay is made up of fourteen 440-foot slabs and eighteen 240-foot slabs with the midpoint of each slab anchored into the subbase with steel dowels. The ends of the slabs are therefore free to slide back and forth in the longitudinal direction with daily and seasonal temperature cycles. As a result, in designing the slab for prevention of temperature cracks, the critical cross-section of the slab is located near the slab midpoint. This concept is discussed in more detail in Ref 6.

To provide maximum prestress at the critical cross-section, the longitudinal tendons were stressed from stressing pockets located near the midpoint of each slab. Two segments of a tendon are anchored at the ends of the slab and overlap within the stressing pocket where they are both post-tensioned simultaneously by use of the lock-coupler. As a result of this central stressing, the loss of prestress due to friction occurs between the midpoint of the slab (where the prestress force is the highest) and the ends of the slab (where the prestress force is the lowest.) The critical cross-section, therefore, feels the highest prestress force, with losses reducing the force in the tendon toward the ends of each slab.

The central stressing also allowed slabs to be placed end-to-end without leaving a gap between them. Previous prestressed pavement projects post-tensioned the tendons from the ends of each slab. This required a gap between slabs, which was later filled in with nonprestressed concrete, referred to as a gap slab. Two joints at a spacing of only 8 feet result from use of the gap slab required by end stressing of adjacent slabs. A more detailed discussion of this point appears in Ref 7.

## TRANSVERSE TENDONS

Tendons in the transverse direction are required to prevent longitudinal cracks from forming under loads and to provide structural integrity between the two lanes of the overlay. Figure 5.1 shows a typical layout of a transverse tendon and the location of the stressing pocket.

The location of the stressing pocket for the post-tensioning of the transverse tendons was chosen for several reasons. One is that a total of four transverse tendons can be stressed with just one post-tensioning operation, which reduces the number of required post-tensioning operations greatly. The second is that the pocket location eliminates many short individual transverse tendons and the many end anchorages which would be required. Other advantages are that slip forming can be used at the edge of the slab and that the stressing pocket is located outside of the traffic lanes. The last reason is that the post-tensioning force required to provide the required level of prestress at the anchored end of the tendons is reduced.

The second point can be illustrated with an example. Figure 5.2 shows a tendon layout with the same length and looped configuration as the tendon in Fig 5.1, the only difference being that the tendon is post-tensioned from one end instead of from a stressing pocket. For this example, the wobble coefficient and the curvature coefficient in Eq 1.1 will be taken as 0.001 and 0.07, respectively. Equation 1.1 is repeated here for convenience:

$$P_s = P_x e^{(Kl_x + \mu\alpha)} \quad (5.1)$$

If a tendon force at the anchored end is required to be 30 kips (i.e.,  $P_x = 30$  kips), the required post-tensioning force,  $P_s$ , can be determined for both tendon layouts. In Fig 5.1,  $l_x = 92$  feet and  $\alpha = 1.5\pi$  radians. Using Eq 1.1, a force,  $P_s = 45.7$  kips, is required. In Fig 5.2,  $l_x = 184$  feet and  $\alpha = 3.0\pi$  radians which results in a  $P_s = 69.8$  kips.

These results show that the use of the stressing pocket reduces the required jacking force approximately 35 percent.

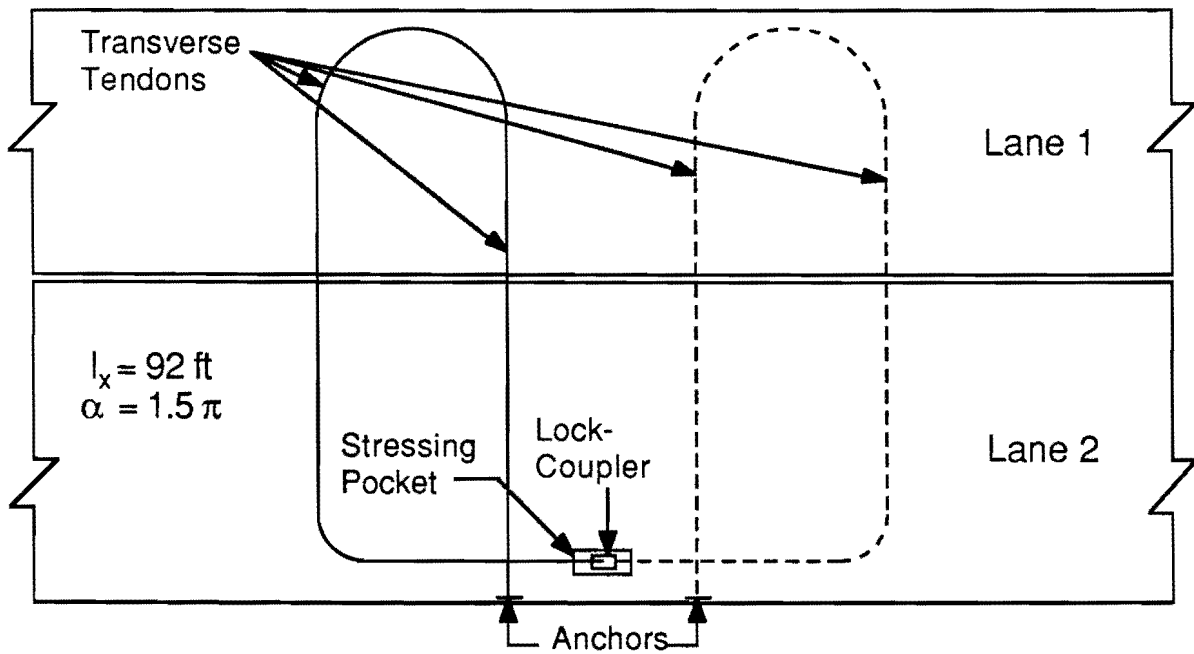


Fig 5.1. Transverse tendons with stressing pocket.

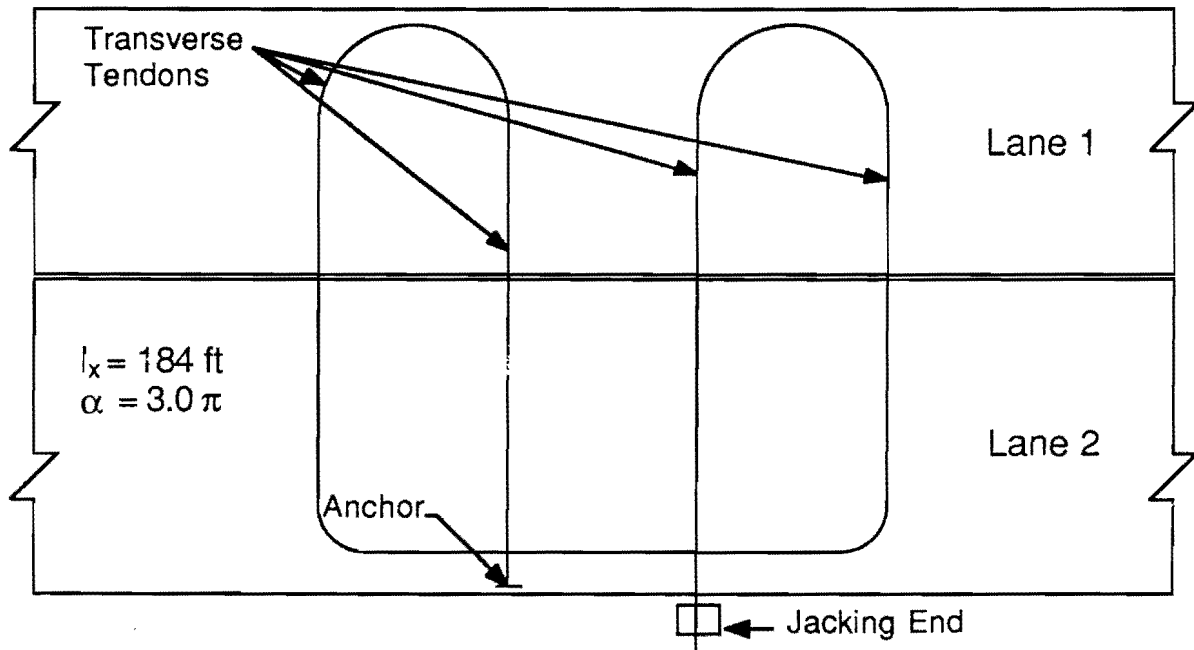


Fig 5.2. Transverse tendons without stressing pocket.

This page replaces an intentionally blank page in the original.

-- CTR Library Digitization Team

## CHAPTER 6. DATA FROM McLENNAN COUNTY OVERLAY

During construction of the prestressed concrete pavement overlay in McLennan County, Texas, measurements were made on 315 longitudinal (straight) tendons and 131 transverse (looped) tendons used in the overlay. For each tendon, the jacking force and tendon elongation were measured. The results from the experimental tests on friction losses were used as guidelines for stressing the tendons in the overlay. The data collected on the overlay were used to determine the actual friction losses and to compare to predicted values.

The overlay consists of 32 prestressed concrete pavement slabs which make up a one-mile stretch of Interstate Highway 35 in McLennan County, Texas. There are two lanes, each made up of seven 440-foot slabs and nine 240-foot slabs. The first lane is 17 feet wide and the second is 21 feet wide. A typical tendon layout for a slab is shown in Fig 6.1.

The tendons were post-tensioned from stressing pockets located at the mid-point of each slab. Lock-coupler devices were used to stress both segments of the tendons simultaneously. The stressing ram used was a VSL type that required a stressing pocket of 10 by 48 inches. The tendons used were plastic coated, 0.6-inch-diameter, 7-wire, low-relaxation strands. These are the same type (Type I) of tendons that were used in the experimental slabs.

The tendon elongations for each tendon were measured as follows:

- (1) Each tendon was stressed to 5 kips to allow seating of the anchors and to take up any slack in the tendon.
- (2) A mark was then made on both segments of the tendon at the exact points where they protruded from the concrete at the edge of the stressing pocket.
- (3) For both segments of the tendon, the distance between the mark on the tendon and the edge of the pocket was measured to the nearest 1/8inch after the final post-tensioning force had been applied. These elongations are relative to the tendon position with 5 kips acting.

The post-tensioning was performed in two stages for each slab. The initial post-tensioning was applied within 12 to 16 hours after casting of the concrete to prevent early cracking of the slab due to shrinkage and temperature cycles. This initial level of post-tensioning was only a portion of the final force level and varied from slab to slab. The final

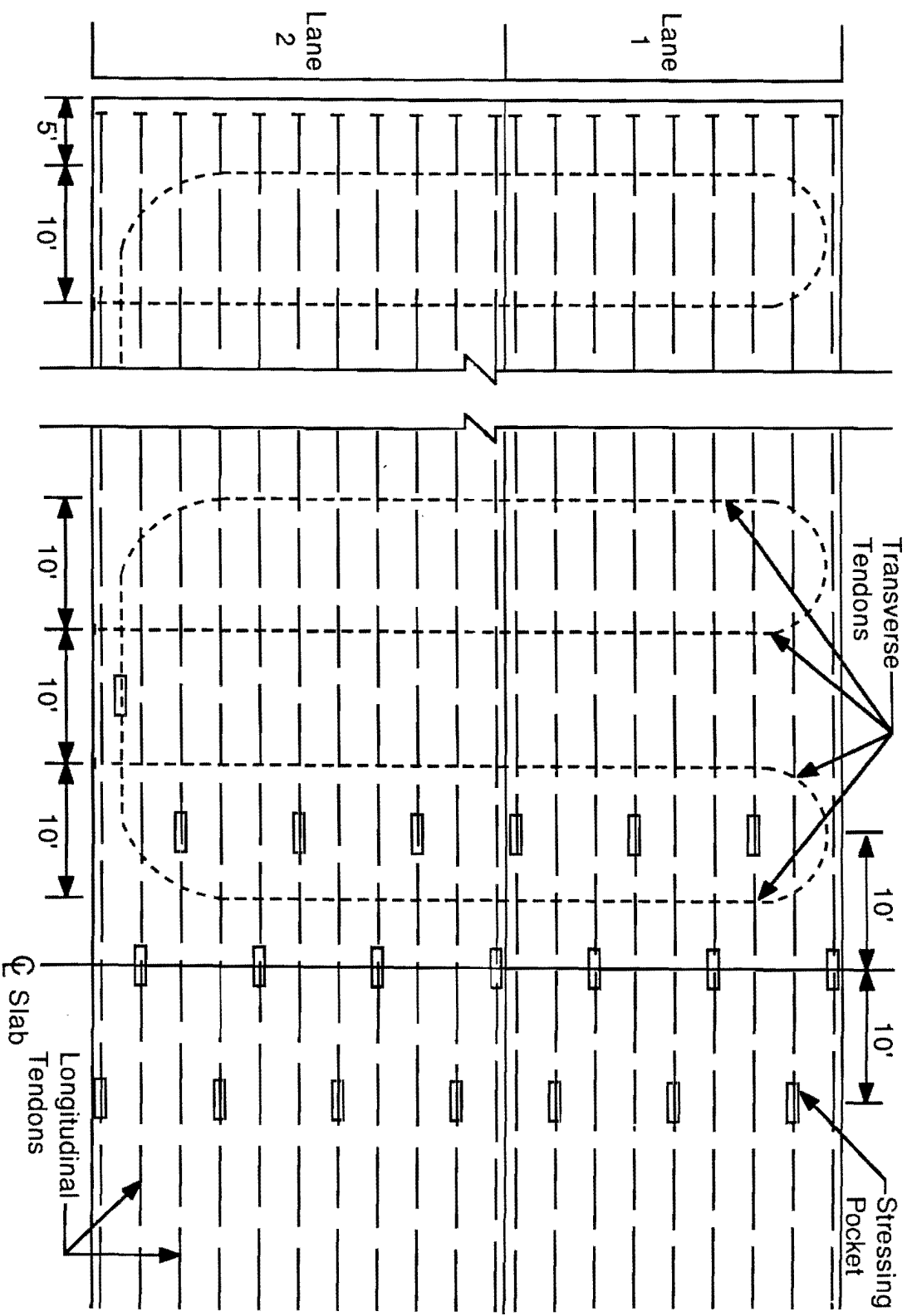


Fig 6.1. Typical tendon layout.

level of post-tensioning was applied once the concrete strength was above the specified strength, typically about three days. Elongations for both levels of post-tensioning were measured relative to the mark made on the tendon at the 5-kip level during the initial stressing. The post-tensioning force was determined from the pressure gauge readings on the calibrated stressing ram supplied by the post-tensioning company.

This page replaces an intentionally blank page in the original.

-- CTR Library Digitization Team

## CHAPTER 7. ANALYSIS AND DISCUSSION OF DATA

The data collected during the post-tensioning operations on the overlay in McLennan County are presented in this chapter, along with the results obtained from an analysis of the data.

### LONGITUDINAL TENDONS

The lengths of the longitudinal tendons vary, depending upon in which slab the tendon is located. In the 240-foot slabs, there are 110, 120, and 130-foot tendon segments, which are connected with lock-couplers at or near the center of the slab. In the 440-foot slabs, the tendon segments are 210, 220, and 230-feet long and are also connected with lock-couplers. A 110-foot segment and a 130-foot segment made up a 240-foot tendon, for example.

The analysis of the data involves separating the measured elongations according to the length of the tendon and the jacking force producing the elongation. The jacking force varies as a result of the different levels of initial post-tensioning that were applied to prevent early cracking of the slabs. A different initial force was used on each slab depending on what stresses the concrete could withstand. The final post-tensioning force was the same for all of the tendons regardless of length ( $0.8 f_{pu}$  results in  $P_s = 46.4$  kips for 0.6-inch, 7-wire tendons).

Tendon elongations for the tendons in the 240-foot slabs are summarized in Table 7.1, according to tendon length and jacking force. Table 7.2 summarizes the elongations for tendons in the 440-foot slabs. All elongations listed are measured relative to the tendon positions with 5 kips acting and are average values for tendons with the same length and jacking force. The jacking forces listed are the forces beyond 5 kips causing the measured elongations. The number of tendons of each length for which data were recorded is also tabulated.

The longitudinal tendons do not go through an intentional angle change, therefore, the friction losses that occur are due only to the wobble friction coefficient. Equation 1.1 can now be written as

TABLE 7.1. TENDON ELONGATIONS, 240-FOOT SLABS

| Jacking<br>Force*<br>(kips) | 110-Foot-Long<br>Tendon |                                  | 120-Foot-Long<br>Tendon |                                  | 130-Foot-Long<br>Tendon |                                  |
|-----------------------------|-------------------------|----------------------------------|-------------------------|----------------------------------|-------------------------|----------------------------------|
|                             | Number of<br>Tendons    | Average<br>Elongation**<br>(in.) | Number of<br>Tendons    | Average<br>Elongation**<br>(in.) | Number of<br>Tendons    | Average<br>Elongation**<br>(in.) |
| 7.4                         | 12                      | 1.21                             | 8                       | 1.44                             | 12                      | 1.47                             |
| 9.7                         | 24                      | 1.64                             | 16                      | 1.91                             | 24                      | 1.99                             |
| 10.8                        | 6                       | 1.83                             | 4                       | 2.12                             | 6                       | 2.25                             |
| 12.0                        | 12                      | 2.13                             | 8                       | 2.28                             | 12                      | 2.47                             |
| 13.1                        | 6                       | 2.42                             | 4                       | 2.47                             | 6                       | 2.65                             |
| 14.2                        | 6                       | 2.60                             | 4                       | 2.94                             | 6                       | 3.23                             |
| 15.3                        | 12                      | 2.82                             | 8                       | 3.10                             | 12                      | 3.28                             |
| 16.5                        | 6                       | 3.10                             | 4                       | 3.17                             | 6                       | 3.46                             |
| 17.6                        | 18                      | 3.28                             | 12                      | 3.63                             | 18                      | 3.94                             |
| 41.4                        | 102                     | 7.68                             | 72                      | 8.57                             | 108                     | 8.43                             |

\* In addition to 5-kip initial force.

\*\* Corresponding to jacking force shown.

Note: There were a total of 138 longitudinal tendons in 240-foot-long slabs, and 36 tendons with 120-foot + 120-foot lengths. All tendons had elongations measured at 41.4 kips jacking force but the data for the elongation at lower force levels was not measured on all tendons

TABLE 7.2. TENDON ELONGATIONS, 440-FOOT SLABS

| Jacking Force*<br>(kips) | 210-Foot-Long Tendon |                               | 220-Foot-Long Tendon |                               | 230-Foot-Long Tendon |                               |
|--------------------------|----------------------|-------------------------------|----------------------|-------------------------------|----------------------|-------------------------------|
|                          | Number of Tendons    | Average Elongation**<br>(in.) | Number of Tendons    | Average Elongation**<br>(in.) | Number of Tendons    | Average Elongation**<br>(in.) |
| 2.5                      | 10                   | 0.70                          | 10                   | 0.65                          | 10                   | 0.71                          |
| 3.5                      | 10                   | 1.08                          | 10                   | 1.10                          | 10                   | 1.16                          |
| 10.2                     | 10                   | 3.51                          | 10                   | 3.59                          | 10                   | 3.69                          |
| 11.5                     | 8                    | 4.00                          | 8                    | 4.19                          | 8                    | 4.39                          |
| 15.3                     | 10                   | 5.39                          | 10                   | 5.69                          | 10                   | 5.93                          |
| 17.9                     | 8                    | 6.22                          | 8                    | 6.42                          | 8                    | 6.64                          |
| 19.1                     | 20                   | 6.60                          | 20                   | 6.84                          | 20                   | 7.03                          |
| 20.4                     | 42                   | 7.06                          | 42                   | 7.36                          | 42                   | 7.79                          |
| 41.4                     | 118                  | 14.63                         | 118                  | 15.11                         | 118                  | 15.33                         |

\* In addition to 5 kip initial force.

\*\* Corresponding to jacking force shown.

Note: There were a total of 177 longitudinal tendons in 440-foot-long slabs, 118 tendons consisting of 210-foot + 230-foot lengths and 59 consisting of 220-foot + 220-foot lengths. All tendons had elongation measured at 41.4 kips jacking force but the data for elongation at lower levels was not measured on all tendons.

$$P_s = P_x e^{-Kl_x}$$

To estimate the wobble coefficient, K, from the collected data, the tendon elongation,  $\Delta l$ , is taken as

$$\Delta l = \int_0^{l_x} \frac{P_x dx}{AE} \quad (7.1)$$

where

$$P_x = P_s e^{-Kl_x} \quad (7.2)$$

- $\Delta l$  = total tendon elongation, feet;  
 $A$  = cross-sectional area of tendon, inch<sup>2</sup>;  
 $E$  = modulus of elasticity of tendon, ksi; and  
 $l_x$  = length of tendon, feet.

Substituting Eq 7.2 into Eq 7.1 and performing the integration leads to the following expression:

$$\frac{K}{(1 - e^{-Kl_x})} = \frac{P_s}{\Delta l A E} \quad (7.3)$$

which can be solved for K knowing the jacking force,  $P_s$ , the total elongation,  $\Delta l$ , and the initial tendon length,  $l_x$ .

The force,  $P_s$ , in Eq 7.3 is taken as the force applied to the lock-coupler device by the stressing ram minus the friction loss through the lock-coupler. This gives the amount of force that actually went into elongating the tendon. As discussed in Chapter 4, the amount of friction loss through the lock-coupler is not precisely known, but varies widely, depending on the condition of the coupler (rusted or unrusted) and the magnitude of the jacking force. The friction loss was assumed to be between 5 and 10 percent of the jacking force.

The wobble friction coefficients calculated using Eq 7.3 are shown in Tables 7.3 and 7.4 for the 240-foot slabs and the 440-foot slabs, respectively. Also shown in the tables are the assumed values of the friction losses through the lock-coupler. These values were based on a percentage of the jacking force estimated from the experimental tests described in Chapters 2, 3, and 4.

#### TRANSVERSE TENDONS

The transverse tendons are all of the same length and did not require an initial post-tensioning as did the longitudinal tendons. Therefore, all of the elongations recorded are for the same final post-tensioning force. As with the longitudinal tendons, the final force and the elongations are measured with respect to the tendon positions with 5 kips acting.

Since the transverse tendons are looped, both the wobble friction coefficient,  $K$ , and the curvature friction coefficient,  $\mu$ , must be considered using the following equation:

$$P_s = P_x e^{(Kl_x + \mu\alpha)}$$

The wobble coefficient is assumed to be the same as the one calculated for the longitudinal tendons, therefore, the curvature coefficient can be determined from

$$e^{\mu\alpha} = \frac{P_s \left( 1 - e^{-Kl_x} \right)}{\Delta l A E K} \quad (7.4)$$

TABLE 7.3. CALCULATED WOBBLE COEFFICIENT, K (240-FOOT SLABS)

| Jacking<br>Force<br>(kips) | Loss in<br>Lock-Coupler<br>(kips) | P<br>s<br>(kips) | 110-Foot Tendons    |                          | 120-Foot Tendons    |                          | 130-Foot Tendons    |                          |
|----------------------------|-----------------------------------|------------------|---------------------|--------------------------|---------------------|--------------------------|---------------------|--------------------------|
|                            |                                   |                  | $\Delta l$<br>(in.) | K<br>(ft <sup>-1</sup> ) | $\Delta l$<br>(in.) | K<br>(ft <sup>-1</sup> ) | $\Delta l$<br>(in.) | K<br>(ft <sup>-1</sup> ) |
| 7.4                        | 0.6                               | 6.8              | 1.21                | 0.0037                   | 1.44                | 0.0019                   | 1.47                | 0.0027                   |
| 9.7                        | 0.8                               | 8.9              | 1.64                | 0.0030                   | 1.91                | 0.0017                   | 1.99                | 0.0022                   |
| 10.8                       | 0.9                               | 9.9              | 1.83                | 0.0030                   | 2.12                | 0.0017                   | 2.25                | 0.0019                   |
| 12.0                       | 1.0                               | 11.0             | 2.13                | 0.0021                   | 2.28                | 0.0023                   | 2.47                | 0.0021                   |
| 13.1                       | 1.0                               | 12.1             | 2.42                | 0.0015                   | 2.47                | 0.0026                   | 2.65                | 0.0025                   |
| 14.2                       | 1.1                               | 13.1             | 2.60                | 0.0017                   | 2.94                | 0.0009                   | 3.23                | 0.0006                   |
| 15.3                       | 1.2                               | 14.1             | 2.82                | 0.0015                   | 3.10                | 0.0013                   | 3.28                | 0.0015                   |
| 16.5                       | 1.3                               | 15.2             | 3.10                | 0.0012                   | 3.17                | 0.0022                   | 3.46                | 0.0019                   |
| 17.6                       | 1.4                               | 16.2             | 3.28                | 0.0013                   | 3.63                | 0.0010                   | 3.94                | 0.0008                   |
| 41.4                       | 3.4                               | 38.0             | 7.68                | 0.0013                   | 8.57                | 0.0008                   | 8.43                | 0.0023                   |

TABLE 7.4. CALCULATED WOBBLE COEFFICIENTS, K (440-FOOT SLABS)

| Jacking<br>Force<br>(kips) | Loss in<br>Lock-Coupler<br>(kips) | P <sub>s</sub><br>(kips) | 210-Foot Tendons    |                          | 220-Foot Tendons    |                          | 230-Foot Tendons    |                          |
|----------------------------|-----------------------------------|--------------------------|---------------------|--------------------------|---------------------|--------------------------|---------------------|--------------------------|
|                            |                                   |                          | $\Delta l$<br>(in.) | K<br>(ft <sup>-1</sup> ) | $\Delta l$<br>(in.) | K<br>(ft <sup>-1</sup> ) | $\Delta l$<br>(in.) | K<br>(ft <sup>-1</sup> ) |
| 2.5                        | 0.2                               | 2.3                      | 0.70                | 0.0031                   | 0.65                | 0.0042                   | 0.71                | 0.0036                   |
| 3.5                        | 0.3                               | 3.2                      | 1.08                | 0.0020                   | 1.10                | 0.0022                   | 1.16                | 0.0020                   |
| 10.2                       | 0.9                               | 9.3                      | 3.51                | 0.0009                   | 3.59                | 0.0011                   | 3.69                | 0.0012                   |
| 11.5                       | 0.9                               | 10.6                     | 4.00                | 0.0009                   | 4.19                | 0.0009                   | 4.39                | 0.0008                   |
| 15.3                       | 1.2                               | 14.1                     | 5.39                | 0.0008                   | 5.69                | 0.0007                   | 5.93                | 0.0007                   |
| 17.9                       | 1.4                               | 16.5                     | 6.22                | 0.0009                   | 6.42                | 0.0010                   | 6.64                | 0.0011                   |
| 19.1                       | 1.5                               | 17.6                     | 6.60                | 0.0010                   | 6.84                | 0.0010                   | 7.03                | 0.0011                   |
| 20.4                       | 1.6                               | 18.8                     | 7.06                | 0.0010                   | 7.36                | 0.0010                   | 7.79                | 0.0008                   |
| 41.4                       | 3.4                               | 38.0                     | 14.63               | 0.0007                   | 15.11               | 0.0008                   | 15.53               | 0.0009                   |

This expression is obtained through an integration similar to the one performed in the previous section.

The values for the measured elongation and jacking force, along with the calculated curvature coefficient, are shown in Table 7.5. To calculate  $\mu$ , the friction loss through the lock-coupler was taken as the value used to calculate K. Also, the wobble coefficient was taken to be 0.001. This value is approximately the one shown in Tables 7.3 and 7.4 for a similar jacking force. Data necessary for calculating  $\mu$  are shown in Table 7.5 also.

#### DISCUSSION OF DATA

The values for the wobble coefficient given in Tables 7.3 and 7.4 cover a wide range. These calculated coefficients are generally higher than the value of 0.001 used to predict the expected elongations, with some values being slightly less. The curvature coefficient was calculated to be slightly higher than the value of 0.07 that was assumed. For all tendons, it was observed that the actual elongations were less than the anticipated ones, and the higher friction coefficients calculated show this.

The most important data are the values of the wobble coefficient at the final post-tensioning force of 41.4 kips. From Tables 7.3 and 7.4 it can be seen that five of the six values for the wobble coefficient, K, are close to 0.001 feet<sup>-1</sup>. Since these values are for the final post-tensioning level, 0.001 feet<sup>-1</sup> should be used for the wobble coefficient in the determination of the required final post-tensioning force, along with a curvature coefficient,  $\mu$ , of 0.089 radian<sup>-1</sup>. The large amount of data obtained provides a good basis for these values.

Factors affecting the analysis of the collected data include the magnitude of friction loss through the lock-coupler and the modulus of elasticity for the tendon. The friction loss assumed was between 5 and 10 percent of the jacking force. This value is an approximation based on the data obtained in the experimental tests and can vary between lock-couplers.

The modulus of elasticity value of 28,000 ksi is used by the manufacturer for the type of tendon used and was obtained from Ref 4. The modulus of elasticity of steel is 29,000 ksi. However, in a 7-wire strand such as the one used in the overlay, the steel wires are wrapped around each other and can twist as the tendon is stressed. If this occurs, larger elongations are

TABLE 7.5. CALCULATED CURVATURE COEFFICIENT,  $\mu$ 

| Jacking Force (kips) | Loss in Lock-Coupler (kips) | $P_s$ (kips) | $\Delta l$ (in.) | $\mu$ (radian <sup>-1</sup> ) |
|----------------------|-----------------------------|--------------|------------------|-------------------------------|
| 41.4                 | 3.4                         | 38.0         | 4.71             | 0.089                         |

$$l_x = 92.0 \text{ feet}$$

$$A = 0.217 \text{ inch}^2$$

$$\alpha = 1.5 \text{ p radian}$$

$$E = 28,000 \text{ ksi}$$

$$K = 0.001 \text{ feet}^{-1}$$

measured than would be if the wires did not twist. How the tendon is stressed determines if it will twist and, thus, how much elongation will occur.

It is important to note that how the tendon is supported during paving operations affects how much unintentional curvature is introduced to the tendon. The tendons in the McLennan County overlay were supported every 3-1/3 feet and were lightly tensioned prior to paving operations. Supporting the tendon in this manner worked well in preventing large displacements of the tendon during paving. The spacing of the tendon supports and the amount of light tensioning needed will vary depending on the size and thus the stiffness of the tendon being used.

## CHAPTER 8. CONCLUSIONS AND RECOMMENDATIONS

### CONCLUSIONS

In the design of prestressed concrete pavements, the effective level of prestressing that the concrete will feel must be determined. The effective prestress level can be determined by knowing how much of the initial prestressing is lost due to friction along the length of the post-tensioning tendon.

Prior to construction of a prestressed concrete pavement overlay in McLennan County, Texas, experimental tests were performed to determine how much friction loss occurs in unbonded post-tensioning tendons. Results from these test were used to predict the friction losses that could be expected in the McLennan County overlay.

The experimental tests were carried out near Valley View, Texas, on four test slabs containing post-tensioning tendons in several different configurations. The tendons tested were plastic coated, 0.6-inch-diameter, 7-wire, low-relaxation strands, which were the type of tendon used in the McLennan County overlay. Also, tests were performed to determine the friction losses generated through the lock-coupler device used to post-tension the tendons within stressing pockets.

As a result of the experimental tests, the following points can be made.

- (1) Tendon flexibility must be considered when looped tendon configurations are used.
- (2) Internally located stressing pockets must be sized so as to accommodate the size of the stressing ram and the anticipated tendon elongation.
- (3) The wobble friction coefficient,  $K$ , and the curvature friction coefficient,  $\mu$ , for the post-tensioning tendons were calculated to be  $0.00145 \text{ feet}^{-1}$  and  $0.0184 \text{ radian}^{-1}$ , respectively.
- (4) The amount of friction loss generated through the lock-coupler device was observed to vary from 2.50 kips to 4.20 kips.

To compute the theoretical friction losses for the McLennan County overlay, the wobble and curvature coefficients were taken to be  $0.001 \text{ feet}^{-1}$  and  $0.07 \text{ radian}^{-1}$ . The friction

losses due to the lock-coupler device were assumed to be taken into account by the wobble and curvature coefficients.

During construction of the McLennan County overlay, measurements of the tendon elongations and the jacking force were taken during post-tensioning operations. The data measured were used to determine the actual friction losses that occurred in the overlay.

The values of the wobble coefficient were observed to be mostly greater than  $0.001 \text{ feet}^{-1}$ , with some values being slightly less. The curvature coefficient was calculated to be  $0.089 \text{ radian}^{-1}$ , which is slightly higher than the  $0.07$  value used to predict the expected elongations. The higher friction coefficients reflect the fact that the actual elongations observed were less than the anticipated ones. It is recommended that, for tendons like the ones used in the overlay, values of  $0.001 \text{ feet}^{-1}$  and  $0.089 \text{ radian}^{-1}$  be used for the wobble coefficient and curvature coefficient, respectively.

During the analysis of the data, it was realized that two factors greatly affected the results obtained for the friction coefficients. The friction loss assumed to occur through the lock-coupler device must be known or reasonably predictable and the modulus of elasticity of the tendon must also be known. The friction loss in the lock-coupler depends on the condition of the coupler (rusted or unrusted) as well as the force in the tendon. The modulus of elasticity of a 7-wire strand will vary depending on whether or not the wires in the strand are allowed to twist during tensioning.

An important point can be made concerning the tendon layouts used in the McLennan County overlay. The central stressing of the longitudinal tendons provides the highest prestress level at the slab midpoint where stresses due to temperature cycles are the most critical. At the ends of the slab, where stresses are due to vehicular loads and not temperature cycles, the prestress level is the lowest (because of friction losses) but still capable of resisting vehicular loads.

## RECOMMENDATIONS

To be able to predict friction losses in post-tensioning tendons more accurately, it is recommended that

- (1) the friction losses through the lock-coupler device be determined with greater certainty, and
- (2) the modulus of elasticity for the post-tensioning tendon be known.

The type of tendon used will determine how much friction loss occurs and tests must be run on each type of tendon to determine the modulus of elasticity.

This page replaces an intentionally blank page in the original.

-- CTR Library Digitization Team

## REFERENCES

1. Mendoza, Alberto, and Neil D. Cable, "Field Tests Conducted Near Valley View, Texas for the Design of the Prestressed Highway Pavement Demonstration Projects in Cooke and McLennan Counties," Technical Memorandum 401-17, Center for Transportation Research, The University of Texas at Austin, September 1984.
2. American Concrete Institute, Committee 318, Building Code Requirements for Reinforced Concrete (ACI318-83), 2nd Printing, September 1984.
3. Chia, Way Seng, Ned H. Burns, and B. Frank McCullough, "Field Evaluation of Subbase Friction Characteristics," Research Report 401-5, Center for Transportation Research, The University of Texas at Austin, May 1986.
4. Post-tensioning Institute, Post-tensioning Manual, 1976.
5. American Concrete Institute, Committee 318, Commentary on Building Code Requirements for Reinforced Concrete (ACI 318-83), 2nd Printing, September, 1984.
6. Mendoza, Alberto, Ned H. Burns, and B. Frank McCullough, "Behavior of Long Prestressed Pavement Slabs and Design Methodology," Research Report 401-3, Center for Transportation Research, The University of Texas at Austin, August 1985.
7. Cable, Neil D., Ned H. Burns, and B. Frank McCullough, "New Concepts in Prestressed Concrete Pavement," Research Report 401-2, Center for Transportation Research, The University of Texas at Austin, August 1985.